AN INVESTIGATION OF THE DEVELOPEMENT OF BED RESISTANCE IN A MOVABLE CHANNEL

By

TANKUT AKALIN

JUNE 1967

ISTANBUL-TURKEY

ACKNOWLEDGEMENT

The author wishes to express his deep gratitude to Prof. Fuat Şentürk for his generous help and guidance.

TABLE OF CONTENTS

LIST OF FIGURES

SYNOPSIS

An investigation has been made on the developement of bed resistance in erodible channels. Types of resistance elements, their formation, importance, old and new aspects of the problem and assumptions of various authors on the subject have been examined. Results of the experiments ran on "Sultan Dere" sand in Devlet Su Işleri Laboratory in Ankara was then evaluated under the light of this theory and two relations were obtained pointing to a jump from ripples to dunes as the flow conditions change and the average velocity increases.

INTRODUCTION

The development of roughness due to different bed configurations is of great importance, because these bed irregularities often contribute the predominant part of the flow resistance. Without the knowledge of these resistances, the behavior of flow can not be predicted with any accuracy.

The appearences of different bed configurations in movable bed channels have been observed and studied extensively by engineers. On the basis of their own data, many investigators have selected as many different parameters to describe the information of these patterns. Yet the causes of various bed patterns are so complex that no generally satisfactory explanation has been found.

The bed pattern changes from one form to another "and quite frequently two different bed patterns, ripples and dunes , for example, appear simultaneously". In these cases, the designation of a certain type of pattern is rather arbitrary. However, from the engineering point of view, the final goal is to find a rational method to estimate the development of frictional resistance at various bed configurations, rather than the variation of the bed geometry itself.

(1) Definitions of Resistance Elements in a Movable Bed Channel

If the roughness is not the same on the sides and the bottom, as is the case for a cross section of a natural river, we can seperate this roughness into two after H. Einstein, as :

U'_* = Friction velocity due to sand particle roughness

U''_* = Friction velocity due to sand particle shape characteristic

$$U'_* = \sqrt{g\, R'\, J} \qquad U''_* = \sqrt{g\, R''\, J}$$

Squaring we get :

$$U_*^2 = U_*'^2 + U_*''^2$$

where :

R' = Hydraulic radius due to sand particle roughness

R" = Hydraulic radius due to sand particle shape

Therefore :

$$R = R' + R''$$

Yet the above relation does not hold for most laboratory channels (including the one in which the experiments of this work have been done) since the sides are not covered with sand. Therefore, the sides and the bottom have different roughnesses. Denoting with subscript t for

bottom and c for sides we can write :

$$U_{*t}^2 = U_{*t}'^2 + U_{*t}''^2 \qquad U_{*c}^2 = U_{*c}'^2 + U_{*c}''^2$$

$$U_{*t}' = \sqrt{g\, R_t'\, j} \qquad U_{*c}' = \sqrt{g\, R_c'\, j}$$

$$U_{*t}'' = \sqrt{g\, R_t''\, j} \qquad U_{*c}'' = \sqrt{g\, R_c''\, j}$$

$$R_t = R_t' + R_t'' \qquad R_c = R_c' + R_c''$$

From semilogarithmic formula it is possible to write :

$$\frac{U}{U_*'} = 5.75 \log 12.27 \frac{R'}{k_s} X \qquad (1)$$

where k_s = specific height of sand particles, and X, a correction factor :

$$X = f\left(\frac{k_s}{\delta}\right) \qquad \text{in Fig. 1-1}$$

$$X = f\left(\frac{k_s\, U_*'}{11.6\, \nu}\right)$$

Vanoni gives a method explained in A-1 to solve for U_*' .(1)

---

(1) Dr.Fuat Şentürk, Akım Formüllerinin münakaşası ve Tatbikati.Teknik Bülten,No:4 September 1965.Ankara,

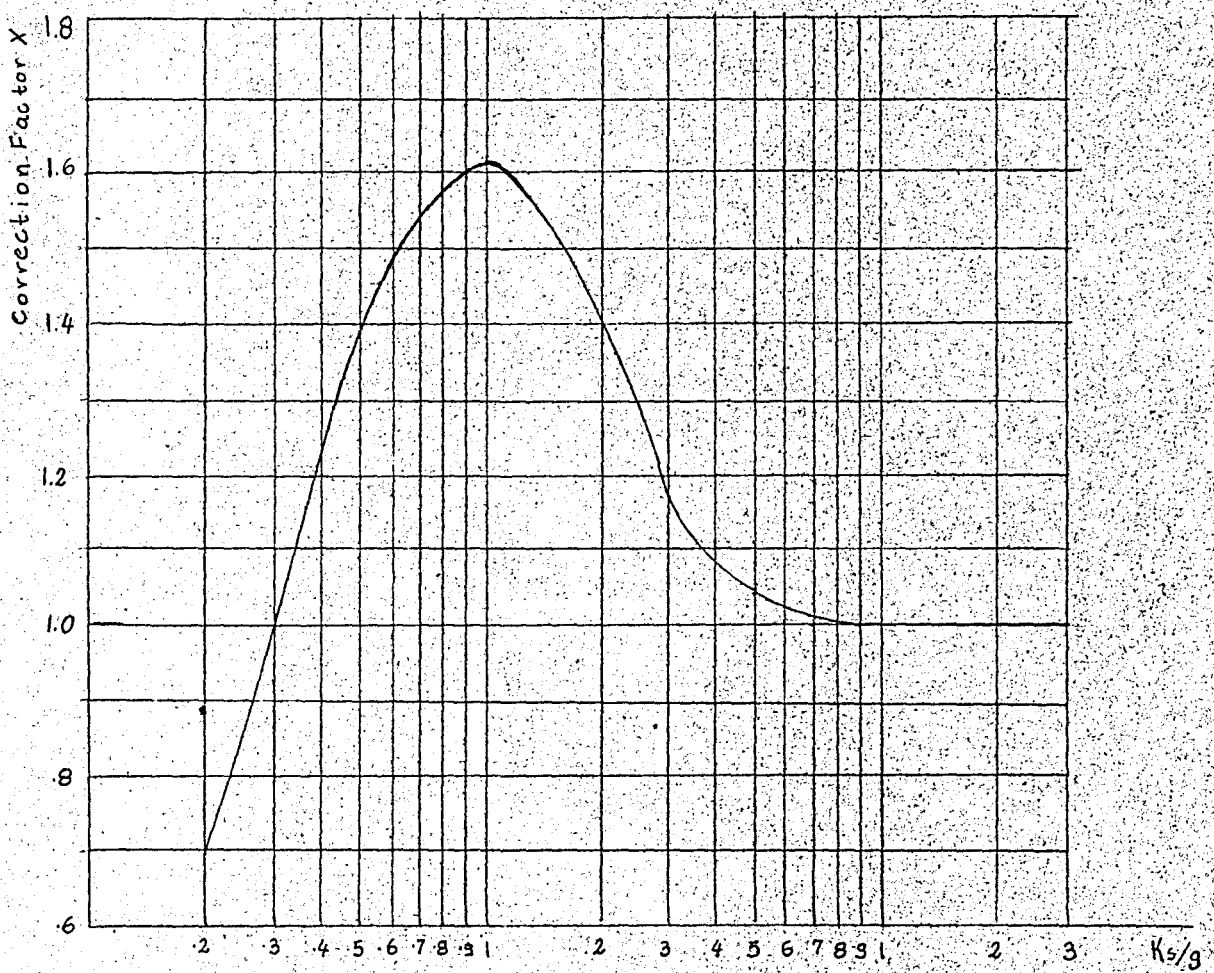
Correction Factor X
1.8
1.6
1.4
1.2
1.0
.8
.6
.2
.3
.4
.5
.6
.7
.8
.9
1
.2
.3
.4
.5
.6
.7
.8
.9
1
2
3
Ks/g

Fig. 1 - 1

Bed Configurations :

When a flow takes place over a movable bed, the bed is first flat, but in time forms and shapes callad bed configurations are formed. These bed configurations can be divided into six, according to Fuat Şentürk (1). These are in the order of the following :

1. Ripples :

When ripples form on a bottom, the free surface of water is not changed, ei. no waves occur on the water. Ripples are three dimensional, and in each coordinate have a different dimension.

Ripple motion is from upstream to downstream. Some of the sand particles proceed from upstream to down stream by saltation.

There is a jump in the resistance to the flow between a plane bottom and a bottom covered by ripples.

When the condition continues to change the resistance of the bottom decreases.

2. Antiripples :

Antiripples have the same characteristics as the ripples, but are larger. When the bottom is covered with antiripples there is a gradual increase in the resistance.

(1) Dr. Fuat Şentürk "Surle Developpement de la Resistance Due Aux Configurations De Fond" - DSI Araştırma Dairesi Başkanlığı - Report No. 318

3. Dunes :

When dunes are formed on a bottom, the free surface of water is covered by small waves.

Dunes are rather bi-dimensional.

The motion of dunes is from upstream to downstream.

Most of the particles in motion is provided by saltation , the sediment transport increases.

The resistance of the bottom increases when the flow conditions change.

4. Wash out :

If flow conditions are changed even further we get wash out with Froude number $S_{fr} = 1$.

5. Antidunes :

Then we pass to supercritical flow with Froude number greater than 1, and get antidunes proceeding from downstream to upstream. The water surface is covered by strong waves. Most grains travel by saltation, and some in suspension.

6. Sand banks :

After antidunes we get sand banks, which is the final type of bed configurations that form in movable bottom channels.

The first of these forms, ripples, antiripples and dunes have been related to each other by Fuat Şentürk in

the following Figure 1-2 :

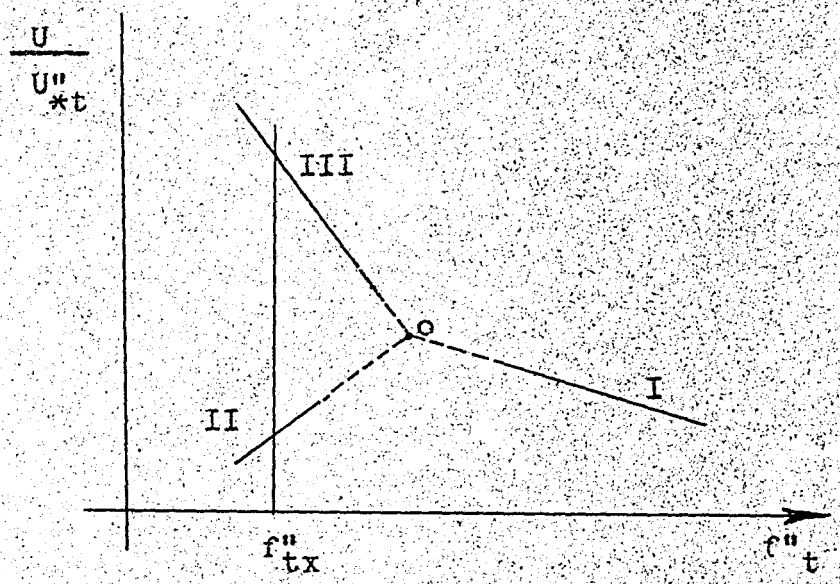

where :

Branch I corresponds to the dunes,

Branch II corresponds to the ripples, and

Branch III corresponds to the antiripples.

As the flow conditions change, and we reach f''_{tx} there is a jump from the ripples to the antiripples.

(2) Geometrical Properties Of Sand Waves

The appearance of sand waves is not incidental. It is an inevitable consequance of flow over a movable bed. Therefore, the properties of the sand waves mustbear certain relationships to the parameters defining the phenomenon. Some recent works on the subject have been performed by Selim Yalin,(1) J.F.Kennedy and A.G.Anderson.

Height Of Sand Waves

Consider a uniform, two dimensional flow(S_{Fr} less than 1)of a real fluid with a free surface over an undulating movable bed. For a bed surface of given size and geometry, this flow can be specified by its depth d, and the average value of the shear stress acting on the bed.

$$\tau_o = \omega j d \qquad (1)$$

Turbulent motion of the fluid is assumed and the velocity of the travel of the sand waves is negligible compared with the average velocity of the flow, which usually is the case. It is further assumed that the three linear quantities of sand wave, length λ, sand wave height H and grain size D are of order

$$\lambda \gg H \gg D \qquad (2)$$

which is usually the casein practice. The validity of eq. 2 implies that , from the point of wiev of fluid motion, the sand waves can be treted as smooth, and the flow picture at the abrupt downstream surface, AB(ie the encircled

region in Fig.2-1), will hardly be effected by the distance Λ. Therefore a flow boundary, ABC, of a given geometrical form, the value of the shear stress τ_B, acting on the lowest point, B can be expressed as:

$$\tau_B = \tau_o f_1\left(\frac{H}{d}\right) \qquad (3)$$

in which $f_1\left(\frac{H}{d}\right) = 1$ if $\frac{H}{d} = 0$. (Because $\theta \simeq$ angle of repose, the geometrical similarity of ABC can be assumed for all granular materials, having approximately the same angle of repose). The value of τ_B must be of the same order as the critical shear stress τ_{cr} corresponding to the fluid and the bed material under consideration, ie.

$$\tau_B \cong \tau_{cr} \qquad (4)$$

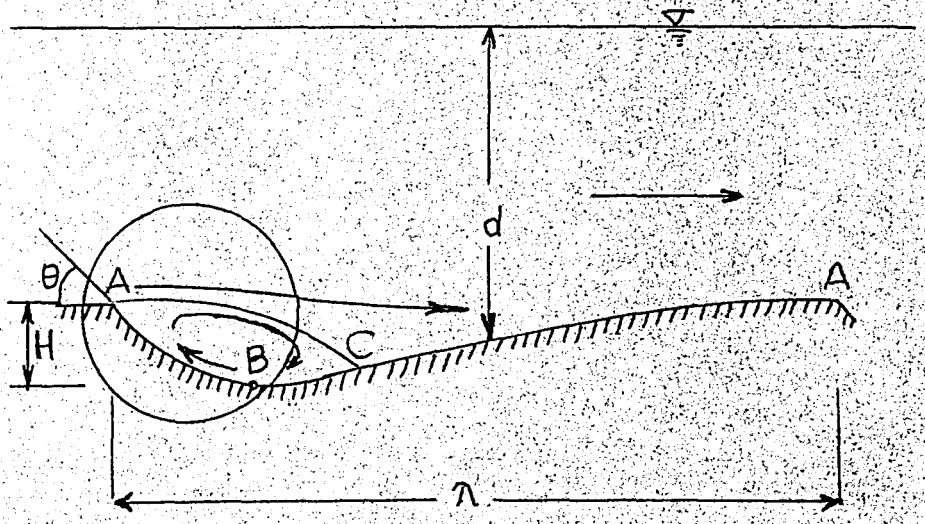

Figure 2-1

This can be explained as follows. The shear stress-

ses acting along AB in the direction B-A cannot prevent a particle from sliding to B, neither can the shear stress to the left of B produce any movements of particles in the direction B-A (although AB is almost horizontal in the vicinity of B). This suggests that the values of the shearstresses acting immediately to the left of B are less than critical. ($\tau_{B,l}$ lessthan τ_{cr}) However, because the sand-waves are travelling without changing shape, continious erosion must take place to the right of B, and this is only possible if the shear stresses in this region are greater than critical ($\tau_{B,r}$ less than τ_{cr}). Thus eq. 4 results because the distribution of shear stresses at B is continious. Substitution of eq. 4 in eq. 3 yields:

$$\frac{\tau_{cr}}{\tau_o} \simeq f_1\left(\frac{H}{d}\right) \qquad (5)$$

or

$$\frac{H}{d} \simeq \phi_1\left(\frac{\tau_o}{\tau_{cr}}\right) \qquad (6)$$

Hence the dimensionless height of a sand wave H/d is a certain function of the dimensionless tractive force, τ_o/τ_{cr}. It must not be assumed from eq. 6 that the value of H is given without considering the properties of the fluid (viscosity μ, and density ρ) and of the bed material (grain size, D, and specific weight of grains in fluid ϖ), because τ_{cr} can only be determined from the Shields curve if the values of all four parameters, μ, ρ, D, and are known. Thus, H/d, being an explicit function of τ_o/τ_{cr}, is an implicit function of μ, ρ, D, and ϖ.

If the variation in τ_o/τ_{cr} is a result of the variation of flow depth, d, only (j = constant) then:

$$\frac{\tau_o}{\tau_{cr}} = \frac{d}{d_{cr}} \qquad (7)$$

then eq 6 becomes:

$$\frac{H}{d} \simeq \phi_1\left(\frac{d}{d_{cr}}\right) \qquad (8)$$

multiplying both sides by d/d_{cr}

$$\frac{H}{d_{cr}} \simeq \phi\left(\frac{d}{d_{cr}}\right) \qquad (9)$$

with

$$\phi = \frac{d}{d_{cr}}\phi_1 \qquad (10)$$

The pattern made by experimental points (S.Yalin's experiments) can be approxim ated by the simple linear form:

$$\phi\left(\frac{d}{d_{cr}}\right) = \frac{1}{6}\left(\frac{d}{d_{cr}} - 1\right) \qquad (11)$$

that is

$$\frac{H}{d_{cr}} = \frac{1}{6}\left(\frac{d}{d_{cr}} - 1\right) \qquad (12)$$

Because of $d/d_{cr} = \tau_o/\tau_{cr}$, the multiplier in brackets on the right side of eq 12 implies the dimensionless excess of tractive force. Thus, the dimensionless sand wave height H/d_{cr}, is proportional to the dimensionless excess of tractive force.

The average of the values of d/d_{cr} corresponding to a flat bed is $\simeq 17.63$. Thus the sand -waves disappear for

$$d/d_{cr} = \tau_o/\tau_{cr} < 17.63$$

Special measurements carried out at the Hydraulic Research Station, England by Selim Yalin gave 15.5 for d/d_{cr}, corr-

esponding to the disappearance of the sand waves.Eq. 12 can be rewritten as :

$$\frac{H}{d} = \frac{1}{6}\left(1 - \frac{d_{cr}}{d}\right) \qquad (13)$$

because $d_{cr} < d$:

$$\frac{H}{d} \lesssim \frac{1}{6} \qquad (14)$$

Thus according to the Eq.12 the height of a sand wave connot exceed 1/6 of the existing flow depth.This result agrees with that given by I.I.Levi obtained from field observations made in various rivers in USSR.

Length Of Sand Waves

At the beginning of a run in which the slope and flow discharge are kept constant,the sand waves form on the initially flat surface of the movable bed,and the flow depth gradually increases.As time passes the depths of erosion h develope(from 0 to H),where as the distance λ ,is observable as soon as the sand waves begin to form,and does not change noticably during the period T.(Selim Yalin) But if λ is already in existance when $h \simeq 0$, then λ must be a certain function of flow over the rough, flat surface at $t = 0$.This has been expressed by Selim Yalin ( ) as:

$$\frac{\lambda}{D} = \phi\left(S_{Rd}, \frac{d}{D}\right) \qquad (15)$$

in which D/d is the relative roughness,and S_{Rd} is the reynolds number related to the grain size, as $S_{Rd} = \frac{U_* D}{\nu}$

In his experiments Selim Yalin(1) got values , that point out to a jump from ripples to dunes. Yet the jump point was not exactly defined.

(3) Resistance Formula In General

From many flow formulas, we shall analyze the three most famous ones. These are:

1) Manning's

$$U = \frac{1}{n} R^{2/3} j^{1/2} \qquad (1)$$

2) Chezy's

$$U = C\sqrt{Rj} \qquad (2)$$

3) Logarithmic

$$\frac{U}{U_*} = A_o + 5.75 \log \frac{R}{k_s} \qquad (3)$$

where:

U = Average Velocity

U_* = Friction Velocity

R = Hydraulic Radius

j = Energy Slope

C = Chezy's Coefficient

k_s = Characteristic Sand Roughness

$\tilde{\omega}$ = Density of water

Taking these one by one and starting with Manning's we see that to get a dimensionally homogeneous equation n should be unitless, yet:

$$n = \frac{R^{2/3} j^{1/2}}{U} = \frac{L^{2/3}}{L/T} = \frac{T}{L^{1/3}}$$

it is not.

Since it is difficult to associate a time unit with a roughness coefficient, U may be written as:

$$U = \frac{\sqrt{g}}{n} R^{2/3} j^{1/2}$$

$$n' = \frac{g}{n} = L^{1/6}$$

Then for convenience sake we set $n' = n$.

If transformed Manning formula may now be written as:

$$\frac{U}{\sqrt{gRj}} = \frac{1}{n\sqrt{g}} R^{1/6} \qquad (4)$$

where $\sqrt{gRj} = U_* =$ Friction velocity. $\therefore$

$$\frac{U}{U_*} = \frac{1}{n} \cdot \frac{1}{\sqrt{g}} R^{1/6} \qquad (5)$$

Solving this for n:

$$n = \frac{1/U_*}{U} 1/\sqrt{g}\, R^{1/6}$$

setting $K = 1/\sqrt{g}$

$$n = \frac{KR^{1/6}}{U_*/U} \qquad (6)$$

On the other hand, solving Chezy's equation for C we see that $C = U/\sqrt{Rj}$. Now checking:

$$C \cdot \sqrt{Rj} = \frac{R^{2/3} j^{1/2}}{n}$$

that is: $$\frac{R^{1/6}}{n} = C \qquad (7)$$

is the connection between Chezy's C and Manning's n. Solving for n and substituting into (6)

$R^{1/6}/C = KR^{1/6}/(U_*/U)$ gives $C = U_*/UK$

Conditions Mannings n depends on :

a. Surface roughness : The surface roughness is represented by the size and the shape of the grains of the material forming the wetted perimeter.

b. Vegetation : Vegetation may be regarded as a kind of surface roughness, but it also markedly reduces the capacity of the channel and retards the flow.

c. Channel irregularity : Channel irregularity is made up of irregularities in the wetted perimeter and variations in cross section size, and shape along the channel length. These may include sand bars, sand waves, ridges, depressions etc.

d. Channel allignment : Smooth curvature with large radius will give a relatively low value of n, where as sharp curvature with severe meandering will increase n.

e. Silting and scouring : Generally speaking silting may change a very irregular channel into a comperatively uniform one and decrease n, where scouring may do the reverse and increase n.

f. Obstruction : The presence of log jams, bridge piers , and the like increases n.

g. Size and shape of channel : An increase in hydraulic radius may either increase or decrease n depending on the condition of the channel.

h. Suspended material : These usually reduce turbulance and appearant channel roughness. This is further discussed in conjunction with Vanoni's experiments.

i. Stage of fater : The depth of water in a channel has a great influence on Manning's n .

Chezy Equation :

$$U = C\sqrt{R.j}$$

The Chezzy formula can be derived from two assumptions :

1. Force resisting the flow per unit area of the stream bed is proportional to the square of the velocity; that is this force is equal to KU^2 , where K is a constant of proportionality. The surface of contact of flow with the stream bed is equal to the product of the wetted parameter and the length of the channel reach or PL. (Fig. 3-1)

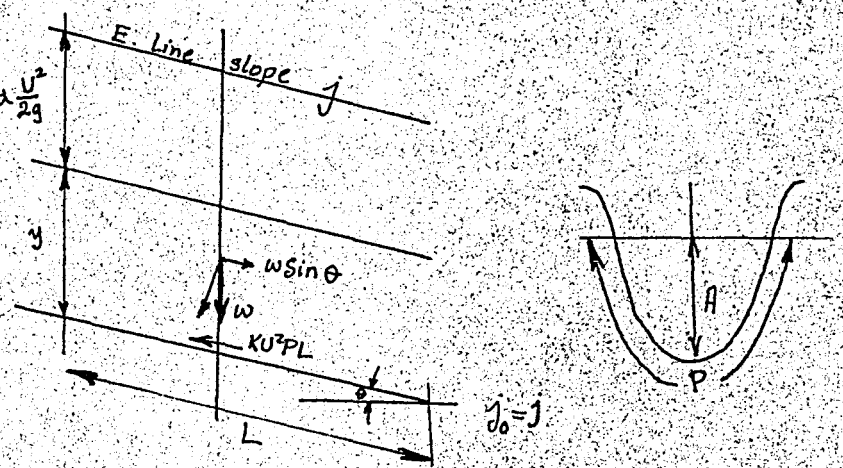

Fig. 3-1

The total force of the flow is then equal to KU^2PL .

2. In uniform flow, the effective component of the gravity force causing the flow must be equal to the total force of the resistance. The effective component of the gravity force is parallel to the channel bottom and is equal to:

$$w\ A\ L \sin\theta = w\ A\ L\ j$$

where:

w = unit weight of water

A = water area

θ = slope angle

j = channel slope

Therefore :

$$w\ A\ L\ j = K\ U^2\ P\ L$$

$$A / P = R \quad \text{and} \quad \sqrt{w/K} = C$$

Then :

$$U = \sqrt{(w/K)(A/P)j} = C\sqrt{R\ j}$$

which is the Chezy formula.

For the value of c various attempts has been made. These are :

a. Kutter Formula :

In 1869, two Swiss engineers, Ganguillet and Kutter published a formula for C :

$$C = \frac{41.65 + \frac{0.00281}{j} + \frac{1.811}{n}}{1 + (41.65 + 0.00281/j)\frac{n}{R}}$$

(in British Units .)

This was experimentally determined from flow measurments data of various types, including Bazin 's gagings . Though the formula appears cumbersome, it usually pro - duces satisfactory results. Widely used, therefore charts have been prepared to save the work.

b. Bazin Formula :

In 1897 French hydraulician H. Bazin proposed a formula for Chezy 's C as a function of R but not of j:

$$C = \frac{157.6}{1+m/\sqrt{R}}$$

(in British units)

where :

m = is a roughness coefficient to which values were pro- posed by H. Bazin.

This formula also depends on experimental results, and usually is less satisfactory than the Kutter formula.

Logarithmic Formulas :

To discuss the logarithmic formula :

$$\frac{U}{U_*} = A_o + 5.75 \log R/K$$

It is useful to look at Prandtl's mixing length theory first.

Prandtl's Mixing Length :

Let us take the simple case of flow parallel to the x axis with :

$\bar{u} = \bar{u}(y)$ $\quad \bar{v} = 0$ $\quad \bar{w} = 0$ and the Shearing Stress :

$$\tau_{xy} = \tau = -\rho \bar{u} v'$$

The fluid particles moving in lumps retain their momentum ll to x. Referring to Fig 3 .2, we assume such a lump from $(y_1 - l)$ layer with a velocity of $\bar{u}(y_1 - l)$ is moved a distance l in the transverse direction. This l distance is Prandtl's mixing length . Since momentum is retained, lumps velocity is less than its surroundings.Then

$$\Delta v_1 = \bar{u}(y_1) - \bar{u}(y_1 - l) = l\,(d\bar{u}/dy)_1 \qquad (1)$$

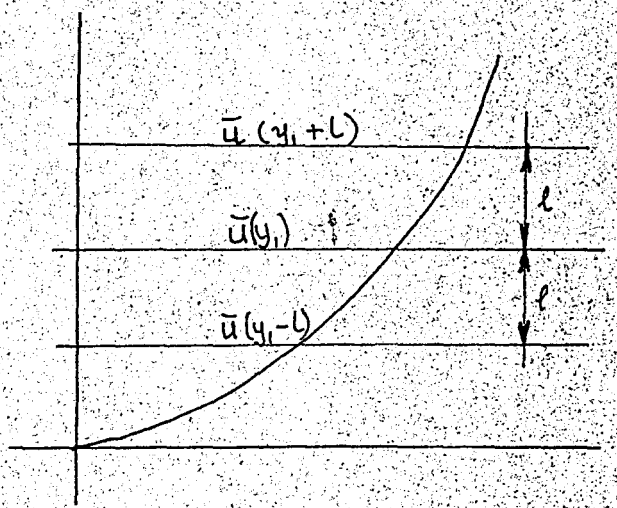

Fig. 3-2

$l(d\bar{u}/dy)$ is obtained from Taylor series with all higher order terms being neglected and v' is greater than 0.

Similarly a lump from the layer $y+l$ has a greater velocity than its surroundings and :

$$\Delta u_2 = \bar{u}\,(y+l) - \bar{u}(y_1) = l(d\bar{u}/dy)$$

with v' greater than 0. These are the turbulent velocity components at y_1. Therefore, we can calculate the time avarage of the absolute value of these fluctuations to get :

$$|\bar{u}'| = 0.5\,(\,|\Delta u_1| + |\Delta u_2|\,) = (\,l\,|d\bar{u}/dy|)_1 \qquad (2)$$

From this, l is defined as : the mixing length is that distance in the traverse direction which must be covered by an agglomeration of fluid particles travelling with its original mean velocity in order to make the difference between its velocity and the velocity in the new layer equal to the new fluctuation in turbulent flow.

Considering two lumps, slower one from (y_1-l) and faster one from (y_1+l) colliding with a velocity 2u' and diverging. These 2 lumps will move apart with a velocity 2u' and the emptying place in between will be filled with other lumps, giving rise to a transverse velocity component in the twodirections at (y_1). From this, we see that, the transverse component of v' is of same magnitude as u', and we get :

$$|\overline{v'}| = \text{Constant} \times |\overline{u'}| = \text{Constant} \times l(d\bar{u}/dy) \qquad (3)$$

It follows from the above presentation that the lumps which arrive at layer y_i with a positive value of v' gives rise "mostly" to a negative $\bar{u}$ so that their product $u'v'$ is negative. For the lumps with negative values, it is vice versa. This results in a negative temporal avarage and :

$$\overline{u'v'} = - c\,|\overline{u'}|\cdot|\overline{v'}| \qquad (4)$$

where: $0 < c < 1$

Combining (2) and (3) we get :

$$\overline{u'v'} = - \text{constant} \times l^2 \,(d\bar{u}/dy)^2$$

or substituting the constant in the mixing length :

$$\overline{u'v'} = - l^2 \,(d\bar{u}/dy)^2$$

which gives the shearing stress as :

$$\tau = \rho l^2 \,(d\bar{u}/dy)^2 \qquad (5)$$

Velocity Distribution in Prandtl's Theory :

Expressing the shear stress as :

$$\sqrt{\frac{\tau}{\rho}} = l\,(du/dy) \qquad (6)$$

we can define :

$$U_* = \sqrt{\frac{\tau}{\rho}} = \sqrt{\overline{u'v'}} = \text{Friction velocity} \qquad (7)$$

Assuming a channel width 2h with the x axis at the middle and coordinate y being measured from the latter; and a constant pressure gradient $(c = \partial\bar{p}/\partial x)$; it will be observed that since $-(\partial\bar{p}/\partial x) + (\partial\tau/\partial y) = 0$, the shearing stress (τ) is a linear function of the width of the channel as :

$$\tau = \tau_o \cdot y/h \qquad (8)$$

with τ_o = stress at the wall

Therefore :

$$\sqrt{\tau_o/\rho} = l \cdot (du/dy)\sqrt{\tau_o/\tau} = U_{*o} \qquad (9)$$

Introducing an empirical dimensionless constant k, Von Karmann made an assumption that :

$$l = -k\,(U'/U'') \qquad (10)$$

On the other hand, Prandtl assumes a proportionality between the mixing length and the wall, near the wall so that :

$$l = ky \qquad (10')$$

then :

$$\tau = \rho k^2 y^2 (du/dy)^2$$

where k is to be determined experimentally, and we get:

$$(du/dy) = U_{*o}/ky \qquad (11)$$

Integrating equation 11 :

$$U = (U_{*o}/k) \ln y + c \qquad (12)$$

Solving for U/U_{*o} :

$$U/U_{*o} = (1/k)\ln y + c \qquad (13)$$

where c is to be determined from the boundary conditions.

Prandtl introduces another assumption as $\tau = \tau_o$; then equation (11) can be written as :

$$U_{*o} = \sqrt{\tau_o/\rho}$$

but at $y = h$, $\bar{u} = \bar{U}_{max}$. Therefore :

$$\bar{U}_{max.} = (U_{*o}/k) \ln h + c$$

$$\frac{\bar{U}_{max.} - \bar{u}}{U_{*o}} = \frac{1}{k} \ln \frac{h}{y}$$

where :

y is the distance from the wall. This is the universal law of Prandtl velocity distribution.

$$\frac{\bar{U}}{U_{*o}} = \frac{1}{k} \ln \frac{y}{y_o} \qquad (14)$$

To determine the constant of integration c from $\bar{U}=0$ at y_o from the wall we see that y_o is influenced by the nature of the wall. Then treating each case seperately :

c for a smooth wall :

y_o is of the order of the magnitude of the laminar sublayer. By dimensional analysis we get :

$$y_o = m\nu/U_{*o} \qquad \text{or}$$

$$m = U_{*o}\, y_o/\nu$$

where U_{*o} is the shear stress near the wall in this section since we are near the wall we shall use U_* instead of U_{*o} .

$$m = U_* y_o/\nu \qquad (15)$$

This is usually called the reduced Reynold's Number. m first defined by Von Karmann is a characteristic of the transition between laminar and turbulent flow. Substitute y_o by

its value in equation 14 , we get :

$$\bar{U}/U_* = 1/k \left(\ln y - \ln m \frac{\nu}{U_*}\right) = a_s + (1/k) \ln \frac{yU_*}{\nu} \quad (16)$$

where :

$$a_s = (1/k) \ln 1/m \quad (17)$$

Nikuradse's experiment showed that k is approx. = 0.40.

Then :

$$\frac{\bar{U}}{U_*} = a_s + \frac{2.30}{0.40} \log \frac{yU_*}{\nu} = a_s + 5.75 \log \frac{yU_*}{\nu} \quad (18)$$

as may be used to compute the value of the friction length.

$$m = e^{-ka_s} \quad (19)$$

as being known, m may be computed now. Again from Nikuradse's experiments we get :

$$\frac{\bar{U}}{U_*} = 5.5 + 5.75 \log \frac{yU_*}{\nu} \quad (19')$$

which is valid for circular pipes with smooth walls. Yet it has been shown by Şahap Aksoy that the use of circular pipe formulas in open channels are accurate within ± 2% and the errors that may arise from the approximate determination of the roughness coefficient n are much larger than this ± 2 % (1).

---

(1) Kenlegan'in Açık Kanallar Hız Formülü Hakkında Bir Eleştirme ve Bütün Enine Kesitler İçin Müşterek Bir Hız İfadesinin Kullanılmasına Dair Teklif. - D.S.İ. Araştırma Dairesi Bşk. - Rapor No. Hi-332

Combining (18) with (19) :

$$a_s = 5.75 \log (1/m) = 5.5 \quad \text{where } k = 0.40$$

$$m = e^{-0.96}$$

$$m = 1/9.2 \simeq 1/9$$

From Eq. (15) :

$$9^{-1} = U_* y_o/\nu \quad \text{and} \quad y_o = (1/9)(\nu/U_*) \qquad (20)$$

Constant c for rough walls :

Only difference is in the roughness height. Therefore again introducing k as a dimensional entity, dimensional analyses gives :

$$y_o U_*/\nu = f(kU_*/\nu)$$

Following the same procedure for the smooth wall case :

$$u/U_* = (1/k) \ln (y/y_o) = (1/k) \ln yU_*/\nu \; \frac{1}{f(kU_*/\nu)}$$

$$u/U_* = (1/k) \ln (yU_*/\nu) - (1/k) \ln f(kU_*/\nu) \qquad (21)$$

writing (21) as :

$$u/U_* = a_r + (1/k) \ln yU_*/\nu)$$

$$u/U_* = a_r + (2.3/k) \log yU_*/\nu)$$

With Prandtl's hypothesis that the shear stress remains constant :

$$U_* = U_{*o} \qquad u_* = U_* \qquad \text{and}$$

$$a_s = (-1/k) \ln f(kU_*/\nu)$$

$$f(kU_*/\nu) = e^{-ka_r} \qquad (22)$$

f can only be determined experimentally and once again, it will be necessary to return to Nikuradse's famous experiments for the interpretation of f. Nikuradse in his experiments used sand with uniform grain size, and changed the diameter of the pipes and the sand particles.

An analysis of Nikuradse's experiments show us that $k_o U_*/\nu \leq 3.63$; a_r is independent of (f); and is constant at 5.5. But 5.5 was measured for smooth pipes. This means that equation (19) is valid for rough pipes, too. i.e. the boundry layer is thick and covers the roughnesses.

The limit 3.63 varies from 3-5 according to various authors.

$$kU_*/\nu \geq 68\text{-}70$$

$$a_r = 8.5 - 2.5 \ln(k_s U_*/\nu)$$

$$a_r = 8.5 - 5.75 \log (kU/\nu) \qquad (23)$$

Then it follows that :

$$u/U_* = a_r + 5.75 \log (yU_*/\nu)$$

$$u/U_* = 8.5 - 5.75 \log(kU_*/\nu) + 5.75 \log (yU_*/\nu)$$

$$u/U_* = 8.5 + 5.75 \log (y/k) \qquad (24)$$

This is the velocity distribution for the rough pipes. A relation may be found if equation (24) is written as :

$$u/U_* = a_r + 5.75 \log (yU_*/\nu)$$

It is then a function of reduced Reynold's number and same form as the equation for smooth pipes. a_r is 6.0 for very wide open channels; 6.25 for usual open channels.

Einstein's Assumptions :

In any type of experimental work some assumptions has to be made in order to idealize the case at hand. The most famous of this type of assumptions applying to the roughness are the ones proposed by H.A. Einstein in "The Bed -Load Function for Sediment Transportation in Open Channel Flows - Technical Bulletin No. 1026 - U.S. Dept. of Agriculture - Washington D.C. - Sept. 1950" as :

1. The cross-section may be divided into two parts, one producing the shear on the bed, and the other the shear on the walls. The boundries between the bed and the wall parts are considered as surfaces of zero shear and are not included in the wetted perimeter of P_t and P_c .
2. The formula for open channel flow between U, U_* , f, and R may be applied to each section as if it were a channel by itself.
3. The avarage velocity and the energy slope in the wall section are equal to the avarage velocity and the energy slope in the bed section, respectively. The roughness of the bed and the roughness of the flume are each homogeneous.

With these assumptions, Einstein obtains the following relationships:

$$\frac{R_c}{f_c} = \frac{4UR_c/\nu}{8R_c j/U^2} = \frac{(4UR_c/\nu)R}{(8R_c j/U^2)R} = \frac{4UR/\nu}{8Rj/U^2} = \frac{S_{Re}}{f}$$

where:

S_{Re}: Reynold's Number

f_c: Frictional resistance due to the banks

U : Velocity in the direction of the main flow

R_c: Hydraulic radius with respect to the banks

j : Energy slope of the flow

ν : Kinematic viscosity

R : Total hydraulic radius

Then, from the data collected from the experiments with water in which :

$$f = f_c = f_t = 8Rj/U^2$$

the curve of f_c vs. S_{Re}/f is obtained, where f_t is the frictional resistance due to thebed.

For the experiments with sediment to be conducted, the values of f_c are read directly from the same curve. To compute R_t:

$$A_T = A_t + A_c = R_t P_t + R_c P_c = RR$$
$$= PfU^2/8gj = P_t f_b U^2/8gj + P_c f_c U^2/8gj$$

but : $Pf = P_t f_t + P_c f_c$

and : $f_t = fP/P_t - f_c P_c/P_t$

where :

A_T : Total cross sectional area

A_t : Cross sectional area pertaining to the bed

A_c : Cross sectional area due to the banks

P : Wetted perimeter

is suggesested by Einstein. Yet, this is quite a long method. Therefore, in our computations, the graphical method of V.Vanani was preferred over the method suggested by Einstein.

For a rectangular channel of width b and debth D where :

$$P = b + 2d$$

$$P_t = b$$

$$P_c = 2D$$

we get :

$$R_t = P(f_t/f) = \frac{R}{f}\left[f+(2D/b)(f - f_c)\right]$$

$$= R\left[1 + (2D/b)(1 - f_c/f)\right]$$

in which :

D : Depth of the water

b : Width of the flume (or river)

The logarithmic law developed by Keulogen is :

$$U/U'_* = 5.75 \log 12.27\, R/k \qquad (1)$$

For a canal with sand roughness only, we can write :

$$U/U'_* = 5.75 \log 12.27\, R'/k \qquad (2)$$

This holds for a characteristic roughness six times the boundry layer ie. :

$$k/\delta = kU_*/11.6\nu > 5.8 \simeq 6$$

For $k/\delta < 6$, a correction to eq. 1 is needed. This correction denoted by x was first given by Einstein as:

$$U/U_* = 5.75 \log (12.27R'/k_s)x \qquad (3)$$

The value of x is given in Fig. 1-1 as :

$$x = f(k_s/\delta)$$

applied with the correction factor as was proposed by Einstein . Eq. 2 yields approximately (approximately, because the points are too much scattered) correct results.

4. Transitions From Varied Regime to Uniform Regime Observed in Movable Bed Channels

It is not possible to obtain uniform flow in natural movable bed channels where Q changes constantly. Yet it is also very difficult to obtain uniform flow in a laboratory flume where Q may be kept constant over a length of time.

To get an idea about the complexity of the problem, let us consider a rectangular flume with sand as bed material and a flow Q. Since the bed will be flat to start with, the initial velocity will be high. Therefore, corresponding depths will be small. But this velocity will soon change the base to ripples or dunes depending on the flow characteristics. Yet to this new roughness with ripples, will correspond a smaller velocity and greater flow depths. As soon as the velocity starts to decrease, and the heights increase, a new base configuration will correspond to this velocity and not to the earlier ripples. Therefore, the ripples will change, too, again affecting the velocity. Therefore, this oscillation (looping) will continue till an equilibrium is reached.

Let us assume a semi-logarithmic flow. Then :

$$U/U_* = 6.25 + 5.75 \log (R/k_s) \qquad (1)$$

where :

U : Average velocity

U_* : Friction velocity

R : Hydraulic radius

k_s : Sand roughness

S_{Fr}: Froude number

j : Hydraulic gradient

$$U/U_* = S_{Fr}/\sqrt{j}$$

Substituting in equation (1) :

$$S_{Fr}/\sqrt{j} = 6.25 + 5.75 \log (R/k_s)$$

$$= 6.25 + 5.75 \log (RU/\nu) - 5.75 \log(k_s U/\nu) \quad (2)$$

If, $S_{Fr}/\sqrt{j}$ vs. $k_s U_*/\nu$ is plotted on a semilog paper, RU_*/ν will give parallel straight lines.

This phenomenon has been explained by Prof. F. Şentürk in two different sections with four phases to a section as follows :(2)

Section I : Bottom Roughness k increasing :

Phase I : Start of the increase in the bottom roughness :

Starting with a flat bottom and a given Q, the bottom will slowly be covered with bed configurations. During the short time in this covering, the flow will not be able to react as fast due to its inertia. That is, k_s will increase while R will remain the same. Therefore, due to R/k_s, $S_{Fr}/\sqrt{j}$ will decrease by a very small amount.

Since R is constant, $S_{Fr} = Q/(A\sqrt{gR}) = \text{Constant}$ in which A shows the wetted cross sectional area. $S_{Fr}/\sqrt{j}$ can increase only if $\sqrt{j}$ is very small. Then, considering

that R= C, j increasing and k_s increasing both

RU_*/ν , U_* , and k_sU_*/ν will increase slightly.

j's variation while R= C cannot be explained and in practice both j and R increase. To get a correct interpretation, both R and j has to be accepted to start changing at the same time.

This corresponds to increasing the resistance; therefore, increasing potential head will be necessary to overcome this higher resistance.

Motion starting is shown by Point 1 in Fig. 4-1.At the end of Phase I we shall be at Point 2. In practice, as k_sU_*/ν increases , so does RU_*/ν depending on U, but this increase,being very slight,has not been shown in the graph but RU_*/ν is accepted as constant. That is why Point 1 and Point 2 are on the same line.

Phase II : When the bed roughness increase reaches the avarage value :

Here k_s, j, U_*, k_sU/ν , RU_*/ν are all increasing. R has also started to increase with a phase lag; but since k_s increases faster than R, R/k_s decrases; the velocity of this decrease starts from 0 and reaches the avarage velocity -m.

With the small increase in R, S_{Fr} starts decreasing. Since R/k_s decreases with -m velocity, so does $S_{Fr}/\sqrt{j}$. This means that j increases with + m velocity. j's velocity being +m, U_* increase velocity, will be + m. Therefore,

$k_s U_*/\nu$'s velocity will reach (+ max.) , while RU_*/ν's reaches (+m). That is, Points 2 and 3 will be seperated due to this velocity difference.

Phase III : Bed roughness velocity reaching a maximum value:

The different parameters affecting the movement are changing in the same directions as in phase 2. The change comes from the velocity of each parameter.

a. R's increase, velocity has reached its avarage value.

b. k_s reaches its maximum velocity. k_s still increases faster than R.

c. Relative roughness continues to decrease with (-m) velocity. Therefore, $S_{Fr}/\sqrt{j}$ decreases with the same velocity. Yet, S_{Fr} is decreasing at the avarage velocity; which means j's increase velocity will decrease and reach zero. Then U_* increases, $k_s U_*/\nu$ reaches its maximum increase velocity. RU_*/ν is increasing,too, but less than the previous case. Point 4 shows this case.

Phase IV : Stop of the increase of bed roughness :

R's increase is comming to a stop while roughnesses has stopped. Therefore, relative roughness increases very slightly, and the bed roughness follows this increase.Slight increase in R causes S_{Fr} 's decrease. Therefore, j decreases.

Since R increases slowly, j decreases with avarage velocity, and therefore the Reynold's numbers.

In Phase 3, S_R was increasing with maximum velocity, and in Phase 4 was decreasing with the avarage velocities, which means a return in the roughness curve. This is under Section 3-4. Checking Fig. 4-1, it can be seen that the decrease velocity of the Reynold's numbers increase. Therefore, the slope of the curve increases. Once this slope reaches its value in Phase 3, it will reverse and start decreasing. The returning curve passes through Point 4. If above this point the flow would gain energy, and if below this point will lose energy. Yet no such state exists. Therefore, the curve passes through Point 4. Point 5 represents this case.

Section II : Bed Roughness k decreases:

Phase V : Start of the decrease in bed roughness :

In Section I, we studied the increase of the roughness. Yet, now the new flow condition does not satisfy the new roughness formed. Therefore, the roughness will start to decrease. Since due to inertia in Section I the roughness (k) increased more than necessary. In Section II, the flow will modify the roughness. Phase V is the start of this new condition. Roughness starts decreasing while R is yet constant. Since velocities are very small, no seperate point has been assigned to it. The increases and decreases are opposite of the ones in Phase I.

Phases VI , VII, and VIII : The different flow conditions due to the decrease in roughness :

These phases are symmetrical with phases II, III, and IV, and are shown with points 6, 7, and 8. At 8, a complete loop has been formed. To reach an equilibrium for uniform flow, these loops will continue getting smaller and smaller. It cannot yet be determined how many loops will be needed before the flow takes its final uniform flow regime.

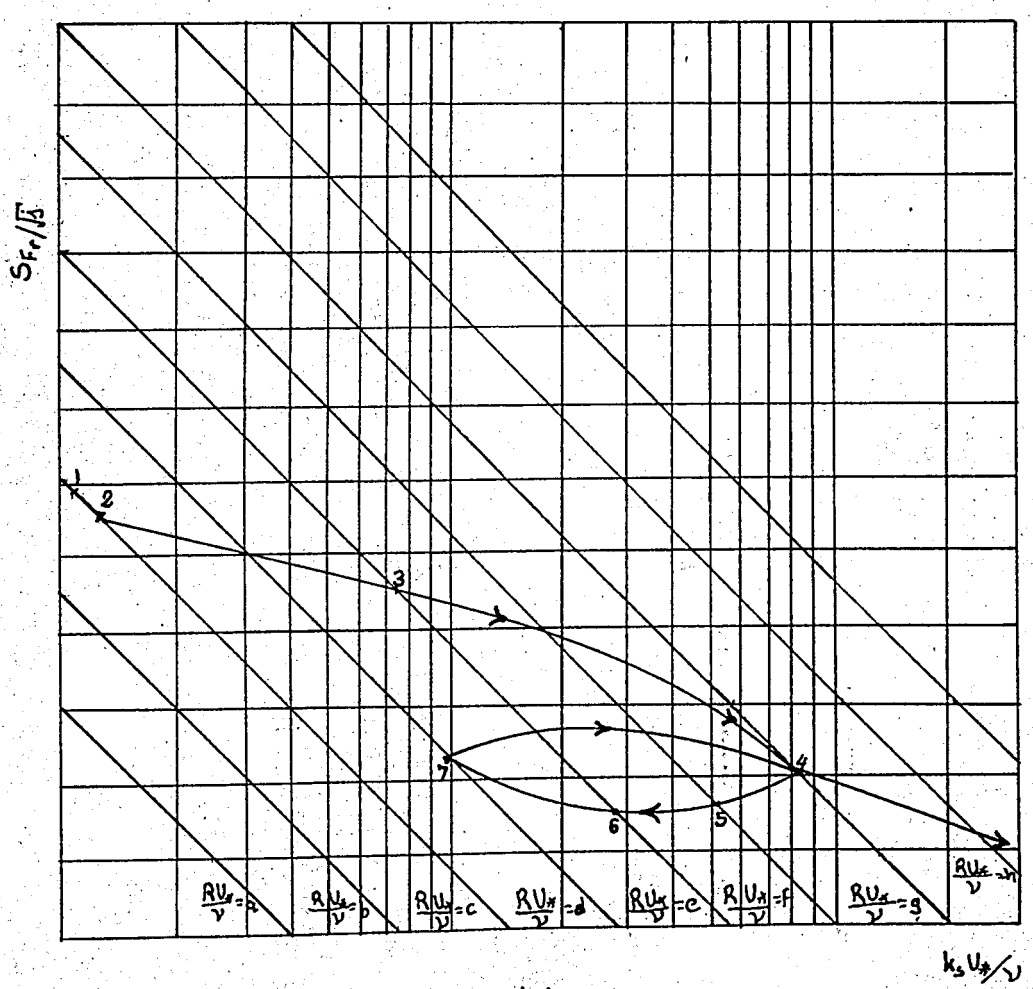

Fig. 4-1

(5) Influence Of Movable Particles On Resistance Formulas

The variation of roughness of sediment laden streams is caused by two distinct processes.

1) Appearance of dunes and bars on the baed which may increase the roughness several times because of the additional resistance and,

2) The damping effect of the suspended sediment on the turbulance, in the stream tending to reduce the hydraulic roughness.

It is difficult to separete the two effects beuse for streams in which a significant amount of bed material is carried in suspension, the two processes are always acting together, but with differing relative effects. For example, in a sediment carying stream flowing at high velocity over a flat bed of sand, the friction factor, or roughness coefficient will probably be lower than that for a clear flow over a fixed bed bed of comparable grain roughness, because of the damping effect of the suspended load. On the other hand, at a lower velocity with light suspended load, dunes may form, and the net result will be an increase in the friction factor over that for a fixed flat bed of the same sand roughness.

Before pointing out V. Vanoni's(3)important work on the subject let us first look at the classical approach.

The reasoning back of the theory of last century

started out by logically assuming the energy head between the stations on a stream, is merely the difference in elevation between the stations.It was then argued that this drop , or head loss, was used up in two ways.

1) In overcoming the hydraulic friction of the flow,

2) In transporting sediment.The more energy used in transporting sediment,the less available to overcome friction , andvice versa.According to Chezy formula , the velocity of a stream is proportional to the square root of the energy slope where the energy slope is merely the loss of energy to overcome friction/unit length of stream.Now , if a turbid stream uses part of the total available energy to transport sediment,it will have a smaller energy slope and hence a smaller velocity than it would have , if it carried no sediment.Thus it was concluded according to Chezy formula a clear stream would flow faster than a comparable one carrying sediment.

Vanoni points out that"Much of the energy to transport sediment comes from the turbulance which itself results from the expenditure of energy in overcoming the friction.Therefore this energy of turbulance is no longer available to overcome friction , and the fact that some of it is used to transport sediment should not necessarily affect dissipation of the main energy head" Also apparently it was not recognized that the friction , or roughness, factor of sediment bearing streams varies widely with load

and flow rate, and that because of this the mean velocity can vary even without a change in energy gradient or depth.

G.K. Gilbert believed in the classical approach too. In his famous flume experiments in sediment transportation expecting to confirm the idea that a clear stream flows with less resistance than a comparable loaded one ,11 out of 16 pairs he selected were to the contrary.As a result of these data Gilbert was forced to admid that the theory was not supported and that there was probably some physical law which escaped his analysis.

Experiments by V.Vanoni(3)in a flume with fixed, artificially roughened bed showed that a flow with suspended load had a smaller friction factor than a clear water flow of the same depth in the same channel.

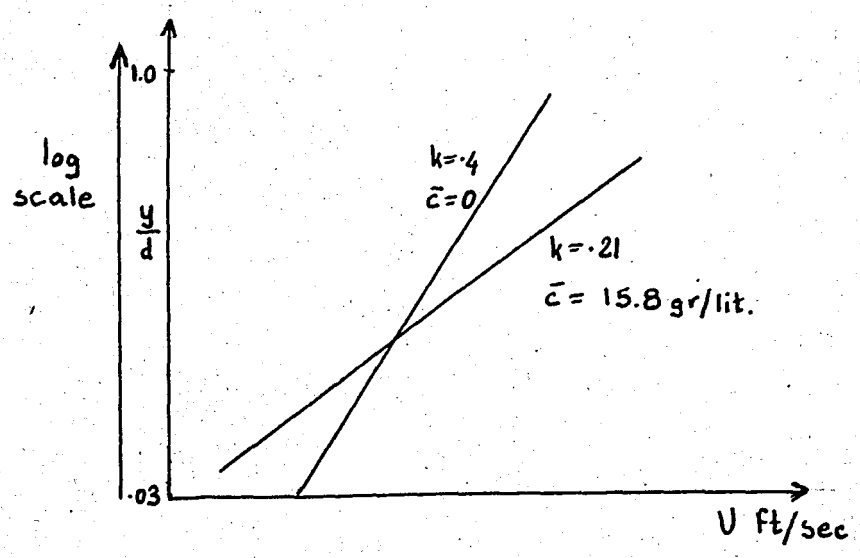

Fig. 5 - 1

The Fig. 5 - 1 above shows velocity profiles at the

center of a flume for two flows of the same slope and depth, one with clear water and the other with a mean concentration ($\bar{c}$) of 15.8 gr/lit of .1mm sediment.

This shows that the velocity profile follows the Von Karmann logarithmic law. For two dimensional flow, profiles can be expressed by:

$$u = \bar{u} + \frac{1}{k}\sqrt{\frac{\tau_o}{\rho}} + \frac{2.3}{k}\sqrt{\frac{\tau_o}{\rho}} \log_{10} \frac{y}{d}$$

where u is the point velocity at y distance up from the bed, $\bar{u}$ is the mean velocity at the profile, τ_o is the shear stress at the bed, ρ is the mass density of the fluid, d is the flow dept , and k is the Von Karmann constant.

The effect of the suspended sediment in reducing k , as indicated by fig. 5 - 1 is a general one which occurs at all times in the laboratory as well as in the field. By adding a sediment load to a flow the friction factor is decreased. The relative magnitude of the reduction in friction factor seems to vary with concentration, the values with highest concentration producing the largest change. Though it appears that rate of change in bed friction factor with concentration decreases at high values of the concentration.

(6) Comparison Between The Resistance Formulas And Their Applications

Manning's formula has a world wide application in uniform flows, it is quite simple to operate with, yet it is noteasy to apply. This is mainly due to difficulties in determining n .nchanges readily from one water stage to another, from one section of water to the next. Therefore the accuracy of the results to be obtained greatly depend on the correct determinationof n. Many tables have been given for n in the literature. Another new method briefly given below is the "Method of Determining Manning's n by Velocity Measurement" which seems to be a promising way of measuring n.

For rough surfaces velocity distribution:

$$U = 5.75U_* \log \frac{30y}{k}$$

depends on the roughness height which may be related to Manning's n.

$$n = \phi \left(\frac{R}{k} \right) k^{1/6}$$

where:

$$\phi\left(\frac{R}{k}\right) = \frac{(R/k)^{1/6}}{21.9 \log(12.2R/k)}$$

That is the roughness in terms of manning's n can be taken as a dominating factor that effects the velocity distribution as:

$$n = \frac{(x-1)y^{1/6}}{6.78(x+.95)}$$

This is the value of n for a wide rough channel with logarithmic velocity distribution. Experiments done so far indicate such a relation but the data is notenough.

The Chezy Formula

$$U = C\sqrt{Rj}$$

presents the same type of problemfor efficient application to uniform flow, correct determination of the coefficient C. Among the attemts made to determine the Chezy C, Kutters C (as disscussed before) is most famous. Though it is hard to use due to its good result yielding, charts have been prepared to determine it graphically, greatly reducing the work associated.

Bazin's C aiming to the same end is not as accurate as Kutters therefoe is not as widely used, though some European countries use it.

The semi logarithmic formula

$$\frac{U}{U_*} = A_o - 5.75 \log \frac{R}{k}$$

when applied with a correction factor(x as Einstein calls it) becomes:

$$\frac{U}{U_*'} = 5.75 \log 12.27 \frac{R'}{k_s} x$$

where

$$x = f\left(\frac{k_s U_*'}{11.6 \nu}\right)$$

As was shown before, the application of this formula gives quite good results.

Generally it should be concluded that since these formulas are either empirical or semi empirical a theoretical comparison is not actually possible. This comparison should be made on an actual river, each quantity calculated by the different formulas and then compared with the actual measurement results.

(7) Interpratation Of Experiment Results

From the experiments run in the rectangular flume in Devlet Su İşleri Laboratory in Ankara (data to which is given in the appendix) some interesting relations were obtained.

In graph 7-1 $\frac{R_t}{R_t''}, j$ versus U/W_{90} is plotted, where:

R_t is the hydraulic radius due to bottom
R_t'' is the hydraulic radius due to sand shape roughness
j is the energy slope
U is the average velocity
W_{90} is the sitting velocity of a D_{90} sand particle

In the beginning of the graph due to very small flow enough points could not be obtained, yet it distinctly shows a decreaing trend. That is in this branch the importance of shape roughness is rapidly increasing. Therefore the value of the fraction R_t/R_t'' decreases. This corresponds to the passage from flat bed to bed configurations and slow formati n of ripples.

Yet as average velocity increases some of the sand particles move in saltation. This , as was explained in connection with Vanoni's experiments decreases turbulance, therefore the apparent roughness. This decrease shows itself as a decrease in the shape roughness. The decrease of the shape roughness therefore the decrease of the related hydraulic radius decreases R_t'' which increases the ratio of $(R_t/R_t'')_j$.

Around $U/W_{90} = 6$ there is asharp jump from ripples to dunes and $(R_t/R_t'')j$ suddenly decreases as dunes form, and R_t'' gets important suddenly. Yet at the velocities invblved, more and more particles get into saltation and some start to travel in suspension, and oneagain result in the

decrease of apparent roughness. This causes the curve to turn upward.

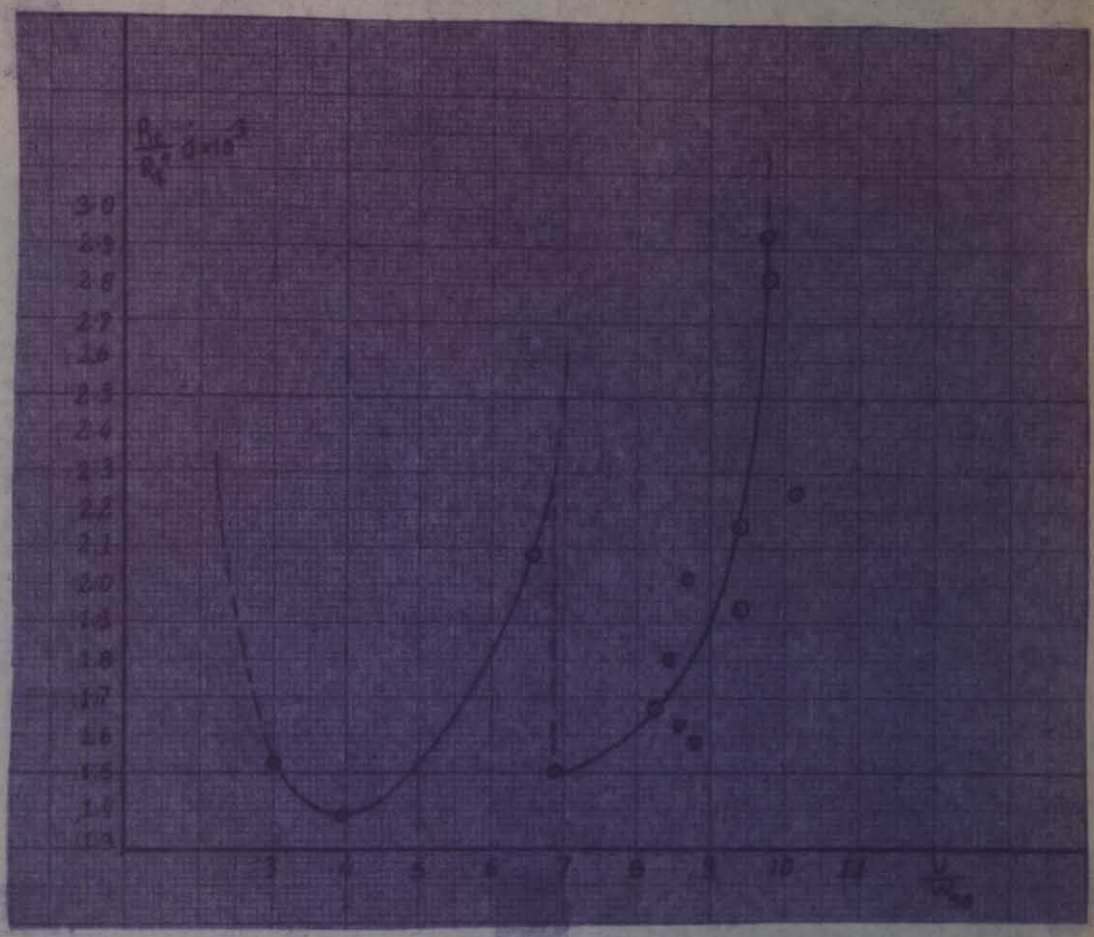

Fig. 7 - 1

decrease of apparent roughness. This causes the curve to turn upward.

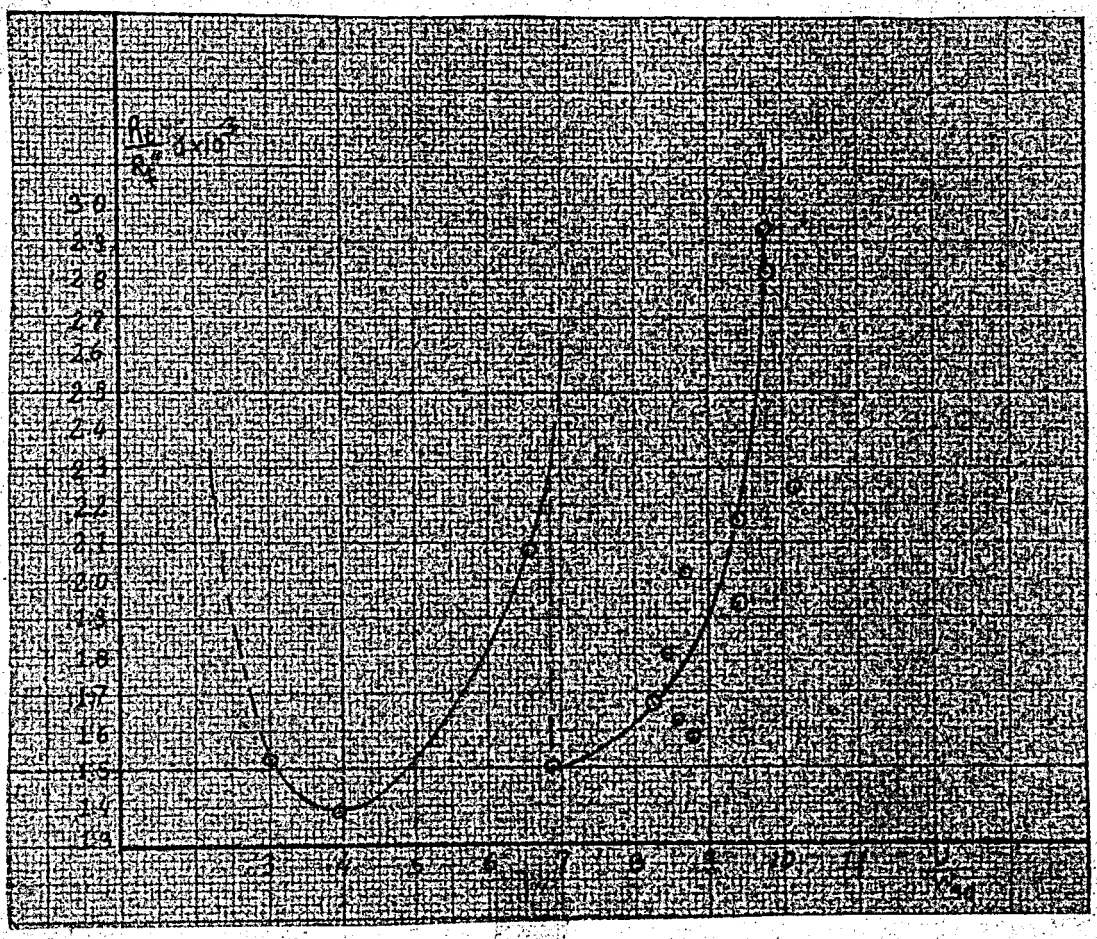

Fig. 7 - 1

In figure 7-2 $\frac{R_t}{R_t'}$ ratio is plotted against the froude number. The results of this figure are very similar to the results of the figure 7-1. The passage from flat bed to ripples, slow decrease of thebottom shape roughness, sudden jump from the ripples to dunes can be seen here too.

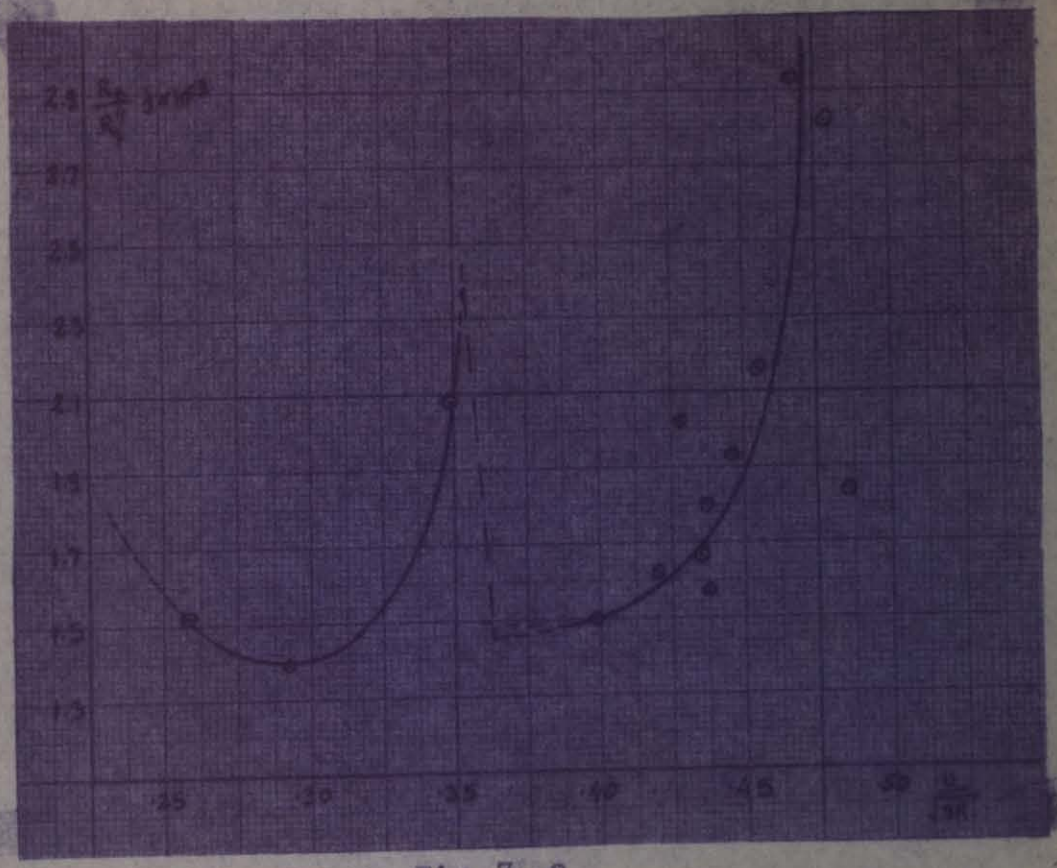

Fig. 7-2

CONCLUSIONS

From the experiments done on sand (specific gravity 2.65) in D.S.İ. Lab in Ankara two resistance relations have been obtained.These experiments point out to a jump from ripples to dunes.Anti ripples didnot take place since the sand used in experiments were finer than the material necessary for the formation of antiripples.Since necesssary flow conditions could not be provided the antidune stage could not be reached either. Howeverin the section done it is shown that the importance of shape roughness varies with the Froude no.transforming from ripples to dunes suddenly, though prior to this sudden change some ripples do form on the back water side of the dunes.

REFERENCES

1) Selim Yalın, Geometrical properties of sand waves, A.S.C.E. Proceedings Journal of the Hydraulic Division, September 1964, pp.105.

2) Dr.Fuat Şentürk, Hareketli tabanlarda üniform akimin teşekkülüne dair, Teknik Bülten sayi 8, Eylül 1966

3) V.A.Vanoni, George Nomicos, Resistance Properties of Sediment Laden Streams, A.S.C.E., Proceedings, Journal of the Hydraulic Division, May.1959 pp:82-84

4) Dr.Fuat Şentürk, Nehir Islahinda Benzeşim, pp:151-157.

5) H.Wen Shen, Developement of Bed Roughness in Alluvial Channels. A.S.C.E. Proceedings, Journal of the Hydraulic Division, May 1962, pp:45-46, 49-52.

6) Ven Te Chow, Open Channel Hydraulics, Chap 8, 1959.

APPENDIX

Calculation Of The Sand And Shape Roughnesses In Practice

In a wide channel with no side effects and with a loose material on the bottom, resistance can be classified in two groups after H.Einstein. These are the sand roughness to which corresponds an R' and shape roughness to which corressponds an R''.

R' and corresponding U_*' can be calculated by V.Vanoni's method. Once R' is determined R'' can be calculated from:

$$R = R' + R''$$

and therefore U_*'' calculated. Since the channel was taken as very wide all these values correspond to the cahannel bottom. Einstein tried to collect these values as :

$$\frac{U}{U_*} = f(\psi)$$

in a diagram. The points are very scattered yet it may be argued that a curve can be obtained. This diagram has not been utilized in practice.

On the other hand if we have a laboratory flume (as is usually the case) we shall have side effects then:

$$R = \frac{A}{X}$$

$$R = R' + R''$$

where

A = Total cross sectional area

X = Total wetted perimeter

R_t = Hydraulic radius corresponding to the channel bottom.

$R_t = R'_t + R''_t$

R'_t = Hydraulic radius corresponding to the sand roughness on the bottom.

R''_t = Hydraulic radius corresponding to the shape roughness on the bottom.

R_c = Hydraulic radius corresponding to the sides.

$$U'_{*t} = \sqrt{gR'_t j} \qquad U''_{*t} = \sqrt{gR''_t j}$$

$$U^2_{*t} = U'^2_{*t} + U''^2_{*t}$$

In a channel with side effects U_* value corresponds to U_{*t} value and this can be calculated by Vanoni's method as shown in appendix A-II. Therefore R_t is known too.

$$R_t = \frac{A}{X} \cdot \frac{f_t}{f}$$

where

f_t = Roughness coefficient corresponding to the bottom.

f = " " " " " section.

Einstein's proposal to these calculations is as follows.

$$A_c = R_c X_c$$

A_c = Virtual wetted section corresponding to the sides.

X_c = Wetted perimeter corresponding to the sides.

A' = Virtual area corresponding to the sand particle

A'' = " " " " " shape

$$A - A_c = A' + A''$$

These values hold for the bottom. Therefore:

$$A' = R_t' (X - X_c) \qquad \text{where}$$

$X - X_c = X_t$ = Wetted perimeter corresponding to the bottom.

$$A' = A - A' - A_c$$

$$R_t'' = \frac{A''}{X - X_c} = \frac{A - R_t' (X - X_c) - R_c X_c}{X - X_c}$$

According to H. Einstein $(X - X_c)$ perimeter holds both for A' and A'' at the same time.

According to Appendix A-II:

$$R_c = R \frac{f_c}{f} \qquad R_t = R \frac{f_t}{f}$$

and from this:

$$\frac{R_t}{R_c} = \frac{f_t}{f_c} = a$$

can be obtained.

$$R_c = R_t . a \quad \text{and} \quad A_c = R_t a X_c$$

substituting $R_t = R_t' + R_t''$ in its place we get

$$R_t = \frac{A - R_t' (X - X_c) - R_c X_c}{X - X_c} + \frac{R_t (X - X_c)}{X - X_c}$$

That is R_t does not depend on R_t'

$$R_t = \frac{A - R_t a X_c}{X - X_c}$$

which means $R_t' = R'$ is assumed. This can be calculated from appendix A-I. In the table given by Vanoni R , R', R'' are not present. Therefore U', R', R'' are not involved in

R_t. That is we can write

$$R_t' = R'$$

This means the sides have an effect on the shape roughness but not on the sand roughness. Therefore

$$XR_t - X_c R_t = A - R_t a X_c$$

$$XR_t - X_c R_t + R_t a X_c = A$$

$$R_t(X - X_c - aX_c) = A$$

$$A = R_t (X - X_c(1 - a))$$

and solving for R_t :

$$R_t = \frac{A}{X - X_c(1 - a)}$$

This value depends on knowing f_t and f_c. Yet in Appendix A-II in the method proposed by Vanoni:

$$R_t = \frac{Af_t}{Xf}$$

It can be shown that these two R_t ' s are the same. Then :

$$\frac{Af_t}{Xf} = \frac{Af_t}{X_t f_t + X_c f_c}$$

On the other hand it was shown in appendix A-II that:

$$Xf = X_t f_t + X_o f_c$$

$$\frac{Af_t}{Xf} - \frac{A}{X_t + \frac{X_c f_c}{f_t}} = \frac{A}{X - X_c(\frac{X_c f_c}{f_t})}$$

then $$X_t = X - X_c$$

Therefore

$$R_t = \frac{Af_t}{Xf} = \frac{A}{X - X_c (1 - f_c/f_t)}$$

Therefore both give the same result. The most important assumption is that $U'_* = U'_{*t}$ .In practice calculation may be done in the sequence below:

1) $U'_* = U'_{*t}$ is found from Appendix A-I

2) R_t " " " " A-II

3) U'_{*t} " " " R'_t

4) R''_t " " " $R_t = R'_t + R''_t$

5) U''_t " " " $U''_t = \sqrt{gR''_t j}$

Appendix A - I

To calculate $U'_* = \sqrt{gR'j}$ I.1

Vanoni proposes the graphical system below: (4)

$$\frac{U}{U'_*} = 5.75 \log 12.27 \frac{R'}{k_s} x \qquad \text{I.2}$$

$$x = f\left(\frac{k_s U'_*}{11.6\nu}\right) \qquad \text{I.3}$$

Substituting x and U'_* into I.2

$$\frac{U}{\sqrt{gR'j}} = 5.75 \log 12.27 \frac{R'}{k_s} f\left(\frac{k_s U'_*}{11.6\nu}\right) \qquad \text{I.4}$$

Where function f is defined in fig 1.1 There are 3 parameters in I.4 as:

$$\frac{U}{\sqrt{gR'j}} \quad , \quad \frac{R'}{k_s} \quad , \quad \frac{k_s \sqrt{gR'j}}{11.6\nu}$$

All parameters contain R'.therefore assigning R' a value and by trial and error a solution may be checked. Yet instead of this trial and error method if we resort to Vanoni's changing parameteres method a short cut may be obtained.Let:

$$\frac{U}{\sqrt{gR'j}} \quad , \quad \frac{U}{\sqrt{gk_s j}} \quad , \quad \frac{U^3}{g\nu j}$$

be the new parameters.A relation can be seen between the old and new parameters.Using these,I.4 becomes I.5 as:

$$\frac{U}{\sqrt{gR'j}} = f_3\left(\frac{U}{\sqrt{gk_s j}} , \frac{U^3}{g\nu j}\right) \qquad \text{I.5}$$

Only R' is known in I.5.Therefore if the parameters not containing R' are evaluated R' can be found.

In I.4 lets change $\left(\frac{R'}{k_s} x\right)$ with its equivalent.

$$\left(\frac{U}{\sqrt{gk_s j}}\sqrt{x} \,/\, \frac{U}{U'_*}\right)^2$$ Then Calculate

$$\frac{U\sqrt{x}}{gk_s j}$$

for different values of U/U'_*. This can be done since U and U'_* are known. $S_R = \frac{U_* k_s}{\nu}$ and therefore from Fig.1.1 x is known. The values obtained are collected on a graph. For the x and $U/\sqrt{gk_s j}$ chosen a U/U'_* will correspond from this graph, and since x is known from fig.1.1 k_s/δ can be found. Therefore:

$$\frac{U^3}{g\nu j} = \left(\frac{k_s}{\delta}\right) 11.6 \frac{U}{U'_*}\left(\frac{U}{\sqrt{gk_s j}}\right)^2$$

Therefore:

$$\frac{U^3}{g\nu j}, \quad \frac{U}{U'_*}, \quad \frac{U}{\sqrt{gk_s j}}$$

are determined. These values are collected on graph AI.1.

Examplele to illustrate thais method.

$U = 1.0$ m/sec. $j: .0001$ $\nu = 10^{-6}$ $k = .010$mm

$$\frac{U}{\sqrt{gk_s j}} = \frac{1}{.1x.01\sqrt{g}} = 320$$

$$\frac{U^3}{g\nu j} = \frac{1}{9.81x.0001x10^{-6}} = 1.02x10^9$$

$U/U'_* = 20.00$ (from fig.1.1) Therefore:

$$U'_* = \frac{1}{19.5} \simeq .05$$

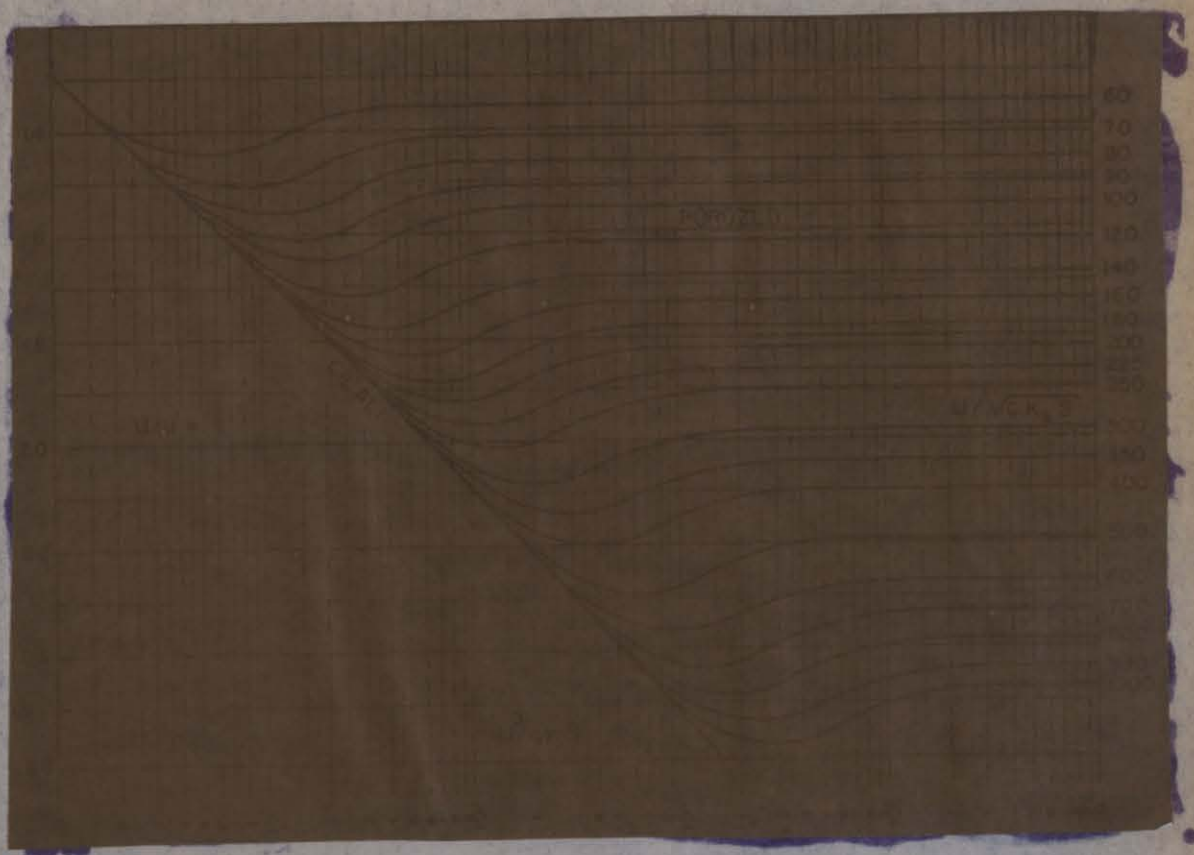

Figure AI-1

Appendix A -II

Vanoni's correction for flume sides. (4)

t : Subscript for bottom

c : " " sides

j : Energy slope

ν : Kinematic viscosity

U : Average velocity

w : wetted crosssectional area

X : wetted cross section

$$R = \frac{w}{X}$$

$U_* = \sqrt{gRj}$ friction velocity II.1

$f = 8(\frac{U_*}{U})^2$ Weisbach friction parameter II.2

$S_R = \frac{4UR}{\nu}$ Reynolds number II.3

Assumptions:

In addition to Einstein's assumptions stated earlier we assume:

side and bottom roughnesses though not the same, are homogeneous.

If in a channel section dimensions: U, j, g, ν, X_c, X_t, are used, X_c and X_t can easily be found and so are R, U_*, f, and S_R. Dimensions to be determined are: U_{*t}, R_t, f_t. Also f_c has to be known. In the given method sides are glass, therefore hydraulically smooth. Threfore simplified. Then relative sand roughness is $= 0$. Then f_c depends only on S_R.

$$S_{R_c} = \frac{4U_c R_c}{\nu}$$

Since $U_c = U$: $S_{R_c} = \frac{4UR_c}{\nu}$ II.4

from which $S_{R_c} = \frac{4UR_c}{\nu}$ and

$S_R = \frac{4UR}{\nu}$ can be obtained by dividing

$$\frac{S_{R_c}}{S_R} = \frac{R_c}{R} \qquad \text{II.5}$$

$S_{R_c} = S_R \frac{R_c}{R}$ is found, but from II.1 and II.2

$$gR_cj = \frac{f_c}{8} U^2 \qquad gRj = \frac{f}{8} U^2 \qquad \text{II.6}$$

is found. If divided:

$$\frac{R_c}{R} = \frac{f_c}{f} \qquad \text{II.7}$$

and from here using II.5

$$\frac{S_{R_c}}{f_c} = \frac{S_R}{f} \qquad \text{II.8}$$

Yet S_{R_c} or f_c can't be determined alone, for this a graph (II.1) is drawn. This depends on Rouse's f as a function of S_R in smooth pipes for Prandtl's "equation in turbulent flow" figure. Then II.8 will give S_{R_c}/f_c and fig. II.1 the value of f_c. Once f_c is known S_{R_c} can be found.

Due to geometrical considerations:

$$w = w_t + w_c \qquad \text{II.9}$$

putting w/X instead of R in II.6

$$w = \frac{XfU^2}{8gj} \qquad \text{II.10}$$

from II.10 $w_t = \frac{X_t f_t U^2}{8gj}$

$$w_c = \frac{X_c f_c U^2}{8gj}$$ is obtained.

From here: $$Xf = X_t f_t - X_c f_c \qquad \text{II.11}$$

for II.9 is obtained. II.11 gives the value of f_t as:

$$f_t = \frac{X}{X_t} f + \frac{X_c}{X_t} f_c \qquad \text{II.12}$$

If the flume is rectangular, then:

$$X = b + 2h$$

$$X_t = X$$

$$X_c = 2h$$

$$f_t = f + \frac{2h}{b}(f - f_c) \qquad \text{II.13}$$

and

$$R_t = R \frac{f_b}{f} \qquad \text{II.14}$$

$$U_{*t} = \sqrt{gR_t j} \qquad \text{II.15}$$

Illustrative example.

$b = 10$ m. $h = 1$ m. $Q = 10\ m^3/sec$ $j = .0009$ $\nu = 10^{-6}$

to find U_t and f_t :

$$w = bh = 10m^2 \qquad U = \frac{10}{10} = 1m^2$$

$$X = 10 - 2.0 = 12 \qquad R = 10/12 = .83$$

$$U_* = (9.81x.83x.0009)^{1/2} = .085$$

$f = 8(.085/1)^2 = .058$ $S_R = \frac{4UR}{\nu} = 3.92x10^6$

to find f_c :

$$\frac{S_{R_c}}{f_c} = \frac{S_R}{f} = \frac{3.92}{5.8} x10^8 = 5.7x10^7$$

from fig. II.1 $f_c = .012$

Once f_c is known f_t can be deteremined as:

$$f_t = f + \frac{2h}{b}(f - f_c) = .058 + \frac{2.1}{10}(.058 - .012) = .0672$$

from which:

$$R_t = R\frac{f_t}{f} = .83x \frac{.0672}{.058} \simeq 1.0$$

$$U_{*t} = \sqrt{gx1x.0009} \simeq .1m/sec$$

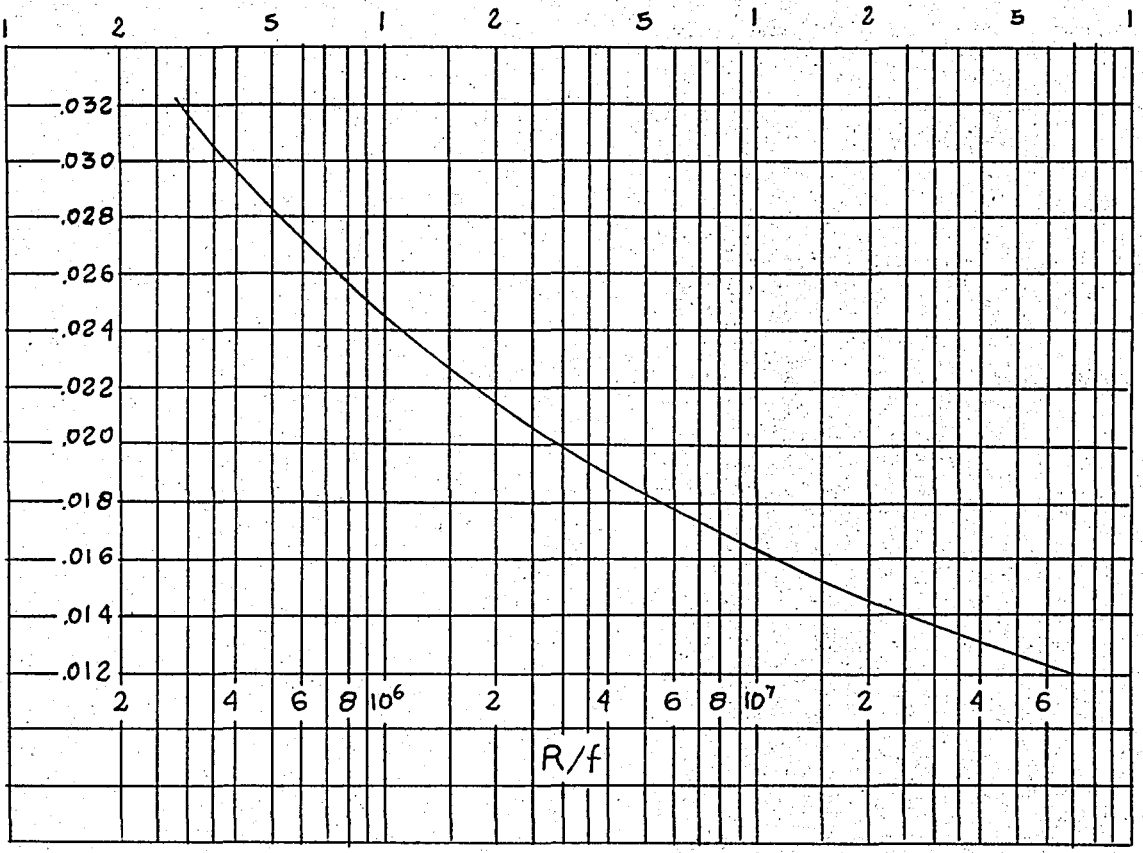
1
2
5
1
2
5
1
2
5
1
.032
.030
.028
.026
.024
.022
.020
.018
.016
.014
.012
2
4
6
8
10⁶
2
4
6
8
10⁷
2
4
6
R/f

Fig. II-1

The Canal Used In Experiments

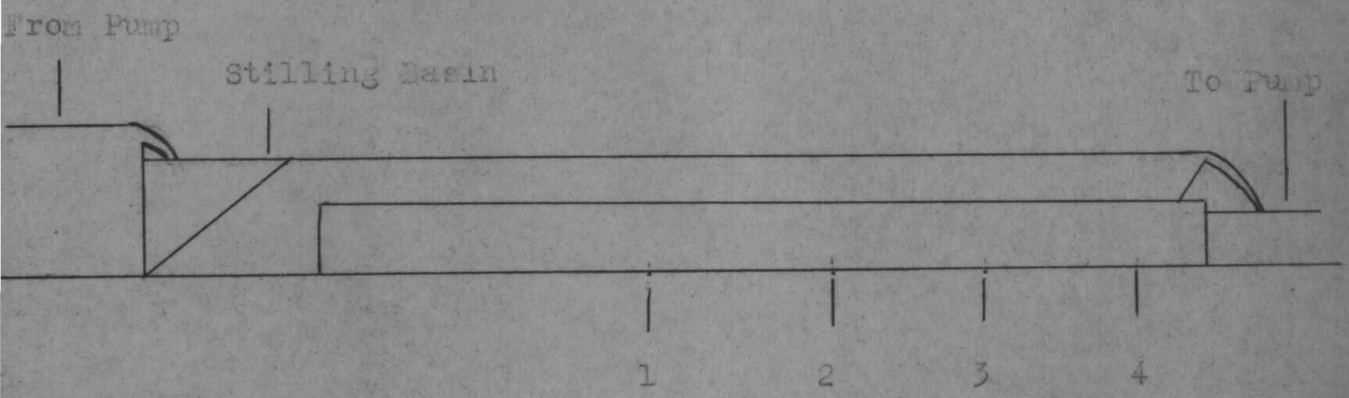

The Characteristics Of The Canal

Length: 57.05m

Width : .90m

Shape : Rectangular

Type : Concrete

The Characteristics Of The Bed Material

D_{10} = .205

D_{35} = .335

D_{50} = .380

D_{65} = .420

D_{90} = .550

D_m = .400

W_{65} = .053 m/sec.

W_{90} = .063 "

Sp. Grav.: 2.61

$\varpi' = \quad = 1.61$

$\varpi' D_{65} = .675$

$P \quad = .266$

No. Of	Q	Temp.	Hook Gage Readings (cm.)				Time	Slope
Exp.	$m^3/sec.$	C°	1	2	3	4		$J \times 10^{-3}$
1	.0112	16	30.06	30.13	29.95	29.48	16:50	1.147
			30.06	30.06	29.90	29.46	17:30	
			30.08	30.08	29.90	29.50	18:00	
2	.0200	18	30.00	30.00	30.00	30.00	11:45	1.030
			31.30	31.20	31.10	31.20	11:55	
			31.50	31.40	31.20	31.35	12:00	
			31.64	31.52	31.40	31.45	12:05	
			31.90	31.80	31.70	31.75	12:15	
			32.10	32.00	31.90	31.90	12:35	
			32.30	32.20	32.10	32.08	13:10	
			32.54	32,45	32.33	32.30	14:00	
			32.72	32.68	32.50	32.33	17:45	
3	.0400	16	35.00	35.00	35.00	35.00	10:25	1.050
			35.34	35.20	35.28	35.30	10:30	
			35.50	35.48	35.40	35.38	10:33	
			36.00	35.97	35.84	35.70	10:42	
			36.20	36.30	35.96	35.80	10:54	
			36.50	36.36	36.16	35.97	11:04	
			36.63	36.50	36.33	36.00	11:27	
			36.63	36.58	36.33	36.00	14:25	
			36.76	36.71	36.50	36.16	14:47	
			36.70	36.62	36.40	36.07	15:10	

No. Of Exp.	Q m^3/sec.	Temp. C°	Hook Gage Readings (cm.) 1	2	3	4	Time	Slope J x 10^{-3}
4	.0700	16	41.20	41.20	41.20	41.20	17:00	1.049
			41.60	41.60	41.45	41.30	17:20	
			41.73	41.65	41.53	41.38	19:55	
			Experi	ment st	opped	and res	tarted	
			41.73	41.65	41.53	41.38	10:00	
			41.82	41.66	41.50	41.54	10:35	
			41.86	41.75	41.62	41.58	11:17	
			41.86	41.80	41.64	41.58	12:00	
5	.1000	16	43.50	43.50	43.50	43.50	16:25	1.081
			43.70	43.70	43.66	43.60	16:35	
			44.10	44.00	43.85	43.82	16:38	
			44.62	44.57	44.40	44.16	16:45	
			45.58	45.30	44.95	44.69	17:05	
			45.40	45.10	44.93	44.69	17:25	
			45.23	45.13	44.87	44.68	18:00	
6	.1100	15.5	45.85	45.85	45.85	45.85	17:15	1.285
			46.63	46.50	46.40	46.33	17:30	
			46.92	46.81	46.68	46.63	17:45	
			47.21	47.00	46.92	46.65	18:20	
			47.10	46.65	46.65	46.65	19:00	
			46.90	46.55	46.53	46.45	19:20	

No.Of	Q	Temp.	Hook Gage Readings (cm.)				Time	Slope
Exp.	$m^3/sec.$	C°	1	2	3	4		$Jx10^{-3}$
7	.1300	16	48.70	48.70	48.70	48.70	16:10	1.190
			49.10	49.04	49.00	49.00	16:15	
			49.40	49.30	49.15	49.15	16:30	
			49.80	49.52	49.23	49.23	16:35	
			50.30	50.00	49.66	49.66	16:52	
			50.42	50.30	49.81	49.81	17:15	
			50.75	50.51	49.90	49.90	17:22	
8	.1500	16	47.40	47.40	47.40	47.40	17:20	1.710
			49.10	49.00	48.62	48.26	17:25	
			50.15	49.74	49.29	48.83	17:30	
			51.37	50.50	49.80	49.30	17:45	
			52.40	51.53	50.20	49.57	17:55	
9	.1600	16	48.80	48.80	48.80	48.80	16:55	1.490
			50.20	49.85	49.90	49.60	17:00	
			52.10	51.70	51.14	50.80	17:10	
			53.00	52.00	51.75	51.00	17:30	
			53.82	52.40	52.30	51.65	17:45	
			54.10	53.50	52.03	51.90	17:50	

No. of Exp.	Q $m^3/sec.$	$\nu \times 10^6$ $m^2/sec.$	R' m.	R'' m.	R''' m.	R_t m.	R_t'' m.	Slope $J \times 10^{-3}$
1	.0112	1.116	.055	.015	.040	.061	.046	1.147
2	.0200	1.080	.075	.022	.053	.085	.063	1.030
3	.0400	1.116	.100	.025	.075	.120	.095	1.650
4	.0700	1.116	.129	.049	.080	.163	.114	1.049
5	.1000	1.116	.145	.064	.081	.184	.120	1.081
6	.1100	1.130	.152	.058	.094	.203	.145	1.285
7	.1300	1.116	.168	.062	.106	.235	.173	1.190
			.166	.050	.116	.238	.188	1.600
			.165	.080	.085	.220	.140	1.000
8	.1500	1.116	.173	.054	.119	.259	.205	1.710
			.169	.045	.124	.248	.203	2.310
			.165	.064	.101	.230	.166	1.620
9	.1600	1.116	.180	.062	.118	.265	.205	1.490
			.176	.043	.133	.266	.223	2.450
			.173	.092	.081	.235	.143	1.130

No. of Exp.	Q m^3/sec.	U'_* m/sec.	U''_* m/sec.	U'''_* m/sec.	U_{*h} m/sec.	U_{*t} m/sec.	U'''_{*t} m/sec.	Slope Jx10^{-3}
1	.0212	.023	.012	.020	.025	.024	.021	1.147
2	.0200	.027	.015	.023	.030	.029	.025	1.030
3	.0400	.040	.020	.035	.046	.044	.039	1.650
4	.0700	.036	.022	.029	.044	.041	.034	1.049
5	.1000	.039	.026	.029	.048	.044	.036	1.081
6	.1100	.044	.027	.034	.054	.051	.043	1.285
7	.1300	.044	.027	.035	.056	.052	.045	1.190
		.051	.028	.043	.064	.061	.054	1.600
		.040	.028	.029	.050	.046	.037	1.000
8	.1500	.054	.030	.045	.069	.066	.059	1.710
		.062	.032	.053	.078	.075	.068	2.310
		.051	.032	.040	.068	.060	.051	1.620
9	.1600	.051	.030	.041	.066	.062	.055	1.490
		.065	.032	.056	.083	.079	.073	2.450
		.044	.032	.030	.056	.051	.040	1.130

No.Of	Q	U	U/U_*	U/U'_*	U/U''_*	U/U_{*t}	U/U''_{*t}	Slope
Exp.	$m^3/sec.$	m/sec.						$Jx10^{-3}$
1	.0112	.190	8.30	15.70	9.50	7.92	9.05	1.147
2	.0200	.250	9.20	15.00	10.90	8.63	10.00	1.030
3	.0400	.346	8.70	17.40	9.89	7.66	8.88	1.650
4	.0700	.432	12.00	19.30	14.90	10.53	12.70	1.049
5	.1000	.520	13.33	20.00	17.93	11.82	14.42	1.081
6	.1100	.532	12.11	19.70	15.68	10.42	12.35	1.285
7	.1300	.539	12.20	20.00	15.40	10.40	12.00	1.190
		.547	10.70	19.50	12.70	9.00	10.10	1.600
		.554	13.80	19.90	19.10	12.00	15.00	1.000
8	.1500	.592	11.00	19.70	13.20	9.00	10.00	1.710
		.616	9.30	19.20	11.60	8.20	9.10	2.310
		.640	12.50	20.10	16.00	10.70	12.50	1.620
9	.1600	.593	11.60	19.50	14.50	9.60	10.80	1.400
		.614	9.40	19.00	11.00	7.80	8.40	2.450
		.632	14.40	19.70	21.10	12.40	15.80	1.130

No. Of Exp.	Q $m^3/sec.$	U m/sec.	U/U^*_h	U'/U''^*	U_t/U''^*_t	U'^2_* $\frac{m^2}{sec^2} \times 10^{-4}$	U''^2_* $\frac{m^2}{sec.} \times 10^{-4}$	Slope $J \times 10^{-3}$
1	.0112	.190	7.60	.600	1.142	1.44	4.00	1.147
2	.0200	.250	8.30	.653	1.161	2.25	5.29	1.030
3	.0400	.346	7.52	.572	1.129	4.00	12.25	1.850
4	.0700	.432	9.82	.730	1.205	4.84	8.41	1.049
5	.1000	.520	10.83	.898	1.221	6.76	8.41	1.011
6	.1100	.532	9.87	.795	1.187	7.30	11.59	1.285
7	.1300	.539	9.80	.772	1.156	7.30	12.22	1.190
		.547	8.50	.651	1.130	7.82	18.46	1.600
		.554	11.10	.865	1.242	7.82	8.40	1.000
8	.1500	.592	8.60	.666	1.118	9.00	20.25	1.710
		.616	7.30	.604	1.103	10.22	28.10	2.310
		.640	10.00	.800	1.177	10.22	16.00	1.620
9	.1600	.593	9.00	.732	1.126	9.00	16.30	1.430
		.614	7.40	.572	1.078	10.21	31.40	2.450
		.632	11.30	1.068	1.275	10.21	9.00	1.130

No.of Exp.	Q $m^3/sec.$	$\frac{U}{W_{65}}$	$\frac{U_*}{W_{65}}$	$\frac{U'_{*t}}{W_{65}}$	$\frac{U'_*}{W_{65}}$	$\frac{U''_{*t}}{W_{65}}$	$\frac{U_{*h}}{W_{65}}$	Slope $Jx10^{-3}$
1	.0112	3.58	.43	.45	.23	.39	.47	1.147
2	.0200	4.72	.51	.55	.28	.47	.57	1.030
3	.0400	6.53	.76	.83	.38	.72	.87	1.650
4	.0700	8.13	.68	.77	.42	.64	.83	1.049
5	.1000	9.82	.74	.93	.49	.90	.91	1.081
6	.1100	10.04	.83	.96	.51	.81	1.02	1.285
7	.1300	10.17	.83	.98	.51	.85	1.06	1.190
		10.32	.95	1.15	.53	1.01	1.21	1.500
		10.44	.75	.88	.53	.70	.94	1.000
8	.1500	11.17	1.02	1.25	.57	1.11	1.68	1.710
		11.62	1.17	1.41	.60	1.28	1.47	2.310
		12.09	.96	1.13	.60	.97	1.21	1.620
9	.1600	11.17	.96	1.17	.57	1.04	1.25	1.490
		11.58	1.23	1.49	.60	1.36	1.57	2.490
		11.93	.83	.96	.60	.76	1.06	1.130

No. Of Exp.	Q $m^3/sec.$	$\frac{U}{W_{90}}$	$\frac{U_*}{W_{90}}$	$\frac{U_{*t}}{W_{90}}$	$\frac{U'_*}{W_{90}}$	$\frac{U'_{*t}}{W_{90}}$	$\frac{U'_{*1}}{W_{90}}$	Slope $Jx10^{-3}$
1	.0112	3.00	.35	.38	.19	.33	.39	1.147
2	.0200	3.96	.43	.46	.24	.40	.48	1.030
3	.0400	6.53	.76	.70	.32	.61	.73	1.650
4	.0700	6.84	.68	.65	.35	.54	.67	1.049
5	.1000	8.25	.62	.70	.41	.57	.76	1.061
6	.1100	8.42	.70	.81	.43	.68	.86	1.265
7	.1300	8.55	.70	.83	.43	.72	.89	1.190
		8.68	.81	.97	.45	.85	1.02	1.600
		8.78	.83	.74	.45	.59	.80	1.000
8	.1500	9.38	.86	1.05	.48	.93	1.42	1.710
		9.77	.98	1.22	.50	1.08	1.24	2.310
		10.15	.81	.95	.50	.82	1.02	1.620
9	.1600	9.39	.81	.98	.48	.87	1.05	1.490
		9.74	1.03	1.25	.50	1.16	1.32	2.450
		10.03	.70	.81	.50	.66	.89	1.130

No. of Exp.	Q $m^3/sec.$	$\tau \times 10^{-4}$	U_*/W_{65}	$k_s \times 10^{-1}$	$\frac{R_t}{R_t'} \cdot j \times 10^{-3}$	$\frac{U}{\sqrt{gR}}$		Slope $J \times 10^{-3}$
1	.0112	.630	.434	.231	1.520	.258		1.147
2	.0200	.773	.509	.315	1.388	.292		1.030
3	.0400	1.650	.728	.420	2.080	.349		1.690
4	.0700	1.352	.654	.542	1.500	.391		1.049
5	.1000	1.538	.708	.603	1.665	.434		1.081
6	.1100	1.354	.830	.638	1.800	.436		1.285
7	.1300	2.000	.830	.705	1.620	.420		1.190
		2.650	.962	.697	2.021	.428		1.600
		1.650	.727	.693	1.570	.435		1.000
8	.1500	2.960	1.020	.726	2.160	.455		1.710
		3.900	1.169	.710	2.820	.478		2.310
		2.675	.962	.693	2.240	.503		1.620
9	.1800	2.682	.962	.756	1.930	.446		1.490
		4.320	1.226	.739	2.930	.467		2.450
		1.954	.830	.726	1.860	.484		1.130

Wave Characteristics

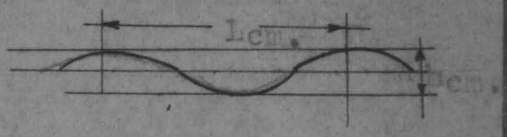

No.Of	0-1		1-2		2-3		3-4	
Exp.	h	L	h	L	h	L	h	L
1	1.6	14	1.5	21	2.0	26	1.0	10
(.0112	1.5	10	3.2	19	1.0	12	1.0	15
m^3/sec.)	2.5	15	1.0	13	1.2	12	3.5	22
	2.0	21	1.3	14	2.0	15	3.5	20
	3.5	21	1.5	16	1.6	18	2.0	19
	3.0	28	3.0	18	2.5	17	3.0	22
	2.0	26	2.2	15	1.0	9	2.5	22
2	3.5	40	2.3	22	1.5	15	2.0	23
(.0200	3.0	28	2.0	12	2.6	18	1.3	23
m^3/sec.)	3.5	30	3.0	13	1.5	16	4.0	25
	1.0	25	2.5	16	3.0	24	1.5	22
	2.0	15	3.0	23	1.5	19	3.0	30
	2.0	26	2.0	14	4.0	31	3.5	25
	1.5	23	2.0	20	2.5	21	2.4	21
3	3.0	43	2.7	20	2.2	18	3.0	17
(.0400	4.5	17	2.4	24	2.6	22	3.0	24
m^3/sec.)	3.0	38	2.0	30	2.0	25	2.2	25

No. Of	0-1		1-2		2-3		3-4	
Exp.	h	L	h	L	h	L	h	L
3	2.0	28	3.0	23	3.0	16	2.0	21
(.0400	3.5	23	5.0	20	2.6	18	3.5	29
m^3/sec.)	2.0	20	2.2	37	4.0	23	2.0	20
	2.8	18	3.5	28	1.0	17	3.0	18
4	6.5	20	4.5	35	3.0	35	4.5	32
(.0700	4.0	31	5.3	45	4.6	36	4.0	31
m^3/sec.)	5.0	45	4.2	28	4.5	30	4.2	32
	7.0	25	4.6	39	3.5	26	4.0	32
	8.0	60	4.7	25	4.5	20	2.5	22
	5.0	80	7.0	24	4.0	13	3.5	18
	6.5	60	4.9	36	4.5	20	5.1	35
5	5.8	53	5.0	58	3.0	27	2.2	41
(.1000	2.5	59	5.3	49	6.0	56	3.0	49
m^3/sec.)	6.0	72	3.5	43	2.8	24	3.2	55
	5.0	56	2.5	34	5.0	28	3.3	42
	5.5	92	3.5	24	2.8	42	2.5	47
	6.0	54	7.0	61	6.0	30	4.5	24
	5.2	58	4.5	71	7.8	64	4.0	27
6	6.0	81	15.0	89	6.5	69	1.5	27
(.1100 m^3/s)	9.0	90	10.0	185	6.0	31	3.0	43

No. Of	0-1		1-2		2-3		3-4	
Exp.	h	L	h	L	h	L	h	L
6	6.2	76	10.0	95	3.5	51	3.5	35
(.1100	10.5	60	6.0	130	7.5	55	10.0	75
m^3/sec.)	4.5	107	11.0	81	4.0	80	8.2	131
	2.0	30	1.0	31	5.0	81	5.3	40
	6.0	30	3.5	20	3.5	28	4.0	105
7	9.5	160	5.0	90	6.5	81	11.5	100
(.1300	7.0	140	12.0	100	7.0	133	6.5	105
m^3/sec.)	6.5	120	9.5	165	6.0	97	7.5	108
	8.0	57	5.5	60	11.0	130	6.0	165
			11.0	122	9.0	108	7.5	90
			5.5	95	10.0	130	7.0	150
			9.5	70	5.5	113		
8	7.5	145	5.0	140	4.0	32	6.0	75
(.1500	6.5	40	6.0	111	8.0	80	6.0	130
m^3/sec.)	17.5	124	7.0	63	10.0	171	9.0	110
	12.0	155	8.0	93	10.5	123	10.0	118
			13.5	106	9.0	137	6.0	52
			7.5	96	10.5	94	8.0	130
			9.0	146	14.0	111	11.0	124

No. Of	0-1		1-2		2-3		3-4	
Exp.	h	L	h	L	h	L	h	L
9	13.0	133	5.0	80	12.0	124	9.0	132
(.1600	13.5	190	12.0	70	10.0	113	9.0	102
m^3/sec.)	11.0	112	7.5	131	9.0	108	10.5	140
	10.0	143	12.5	150	3.5	66	10.0	128
	8.0	85	9.0	110	12.0	140	14.0	102
			14.5	150	9.0	160	7.5	130
			11.5	90	10.5	154	16.0	113